Isar II, a 500 kJ double-fed linear Theta-Pinch

G. Klement, A. Knobloch, R.C. Kunze
G. Nützel, H. Schlageter

IPP 4/58 June 1968

INSTITUT FÜR PLASMAPHYSIK
GARCHING BEI MÜNCHEN

INSTITUT FÜR PLASMAPHYSIK

GARCHING BEI MÜNCHEN

Isar II, a 500 kJ double-fed linear Theta-Pinch

G. Klement, A. Knobloch, R.C. Kunze
G. Nützel, H. Schlageter

IPP 4/58 June 1968

The contents of this report will be presented at the Fifth Symposium on Fusion Technology, Oxford, England 2nd - 5th July 1968.

Die nachstehende Arbeit wurde im Rahmen des Vertrages zwischen dem Institut für Plasmaphysik GmbH und der Europäischen Atomgemeinschaft über die Zusammenarbeit auf dem Gebiete der Plasmaphysik durchgeführt.

IPP 4/58

Isar II, a 500 kJ double-fed linear Theta-Pinch

G. Klement, A. Knobloch,
R.C. Kunze, G. Nützel,
H. Schlageter

Juni 1968

Abstract

Two half-banks of 250 kJ each are discharged into a double-fed coil. This design allows the high frequency of about 90 KHz and a better symmetry of the magnetic field configuration.

The experiment can be run with partial energy (steps of 20% of the maximum), where for every possible energy step the feed of the current is axisymmetric with respect to the minor axis for a linear coil and point symmetric for a single fed torus. Making the collector width equal to the coil length in the linear case, any change from a linear coil to a toroidal one will be relatively easy. The geometrical design of the installation was governed by these features.

In order to get close package of the load cables at the load plug in contacts were developed.
The arrangements of the complete installation and the auxiliary units, which were determined by the spetial conditions, are described. The experiment is equipped with a premagnetisation bank and a Theta-Pinch preionisation unit.
The assembling of the banks and, in some cases the manufacture of some components has supervised with the aid of job planning techniques.

The experince with these techniques will be discussed.

The main data of the installation are:

Bank	2 x 250 kJ
Voltage	2 x 40 kV
Peak current	7,1 MA
Frequency	90 KHz
Peak flux density	89 KG
Initial rise of flux density	50.5 kg/μs
Coil length	100 cm
Coil bore diameter	10 cm

1. Introduction

This report is on a new fast capacitor bank of Theta-Pinch experiments in the Institut für Plasmaphysik in Garching. The installation has now been finished and is now in operation.

2. Requirements and their consequenses

The special disposition of the installation and the mechanical design of the single components, were strongly influenced by the requirements of the experiment:

2.1 The installation should be able to feed two different loads, namely a linear coil and a toroidal one for which the installation should be able to be changed with parably small expenses.

2.2 The required fast current rise in the linear experiment (discharge frequency about 100 kHz) is achieved by series connection of two bankhalves. The coil will be double-fed in this arrangement, the two bank halves being arranged symmetrically with respect to the coil axis.
The double fed coil has the advantage of a better magnetic field symmetry.

2.3 With respect to a Limpus-experiment it was required, that the two bank halves should be divided into fifths. The bank is charged via 2 x 5 disconnecting switches; the triggering of the start gaps and the crowbar gaps requires 2 x 5 submaster gaps and 2 x 5 Marx-generators respectively.
The coil is fed via 2 x 5 precollectors in such a way that, even for partial performance of the bank halves, a symmetrical feed results for the linear coil as well as for the torus. An interlocking system controls that both bank halves operate at equal partial energy and furthermore is symmetrical feed of the coil.
The requirements concerning operation at partial energy determines the technical outlay of auxiliary equipment and control system.

2.4 The possibility mentioned of changing the experiment from a linear to a toroidal coil is easily given since the collector width corresponds to the coil length. All 20 precollectors have the same form, thus for a change of the coil only the transition between precollectors and coil has to be replaced.
The precollector arrangement is a concentric one for a Torus-experiment whereas with the double-fed coil the precollectors are arranged in two packages, one package being revolved by 180° in order to get the correct series connection of the bank halves. The pulse cables connecting the bank and precollectors have 3 different lengths and can be used for the toroidal and the linear arrangement.

2.5 The capacitor bank can be enlarged by 60 %. This possibility was also considered in the arrangement of the auxiliary equipment. Since in the linear experiment the collector width is equal to the coil length, the load-system can be enlarged as required.

2.6 The installation includes two auxiliary banks, namely a bias field bank and a Z-Pinch preionisation bank. A further auxiliary bank, a Theta-Pinch preionisation, is in the development state.

The bias field bank has been subdivided, as was the main bank, for the preionisation banks subdivision is not necessary.

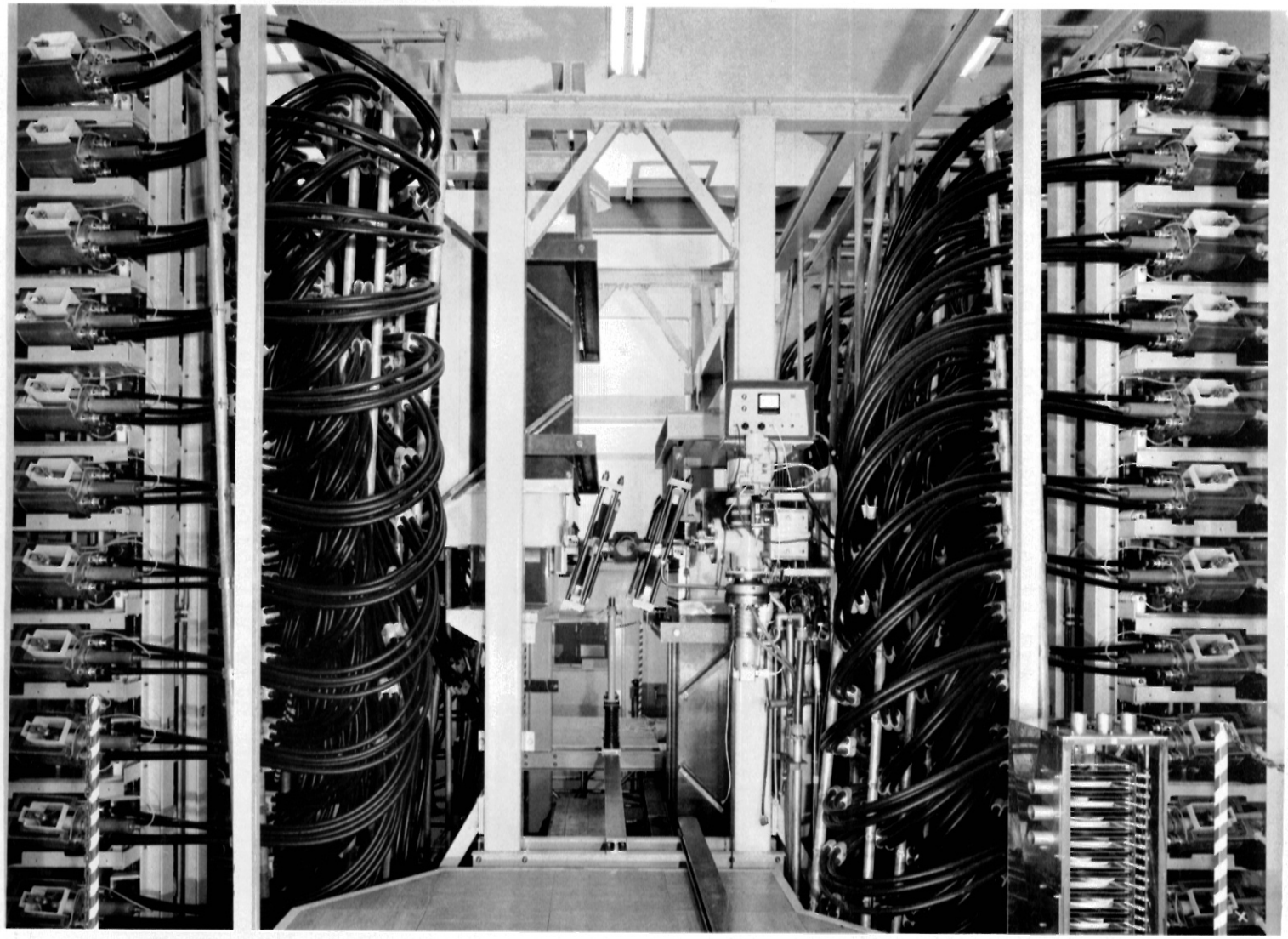

P 124 500 kJ - Theta - Pinch Isar II

Main bank, collector system with double-fed linear coil

3. Arrangements of main bank, collector system, coil and auxiliary units

Isar II is been mounted in one of our experimental buildings, which has a free height of about 5 meters, and a base area of 12,2 x 10,3 meters. The corresponding basement room could also be used for the installation. Control and monitoring of the system as well as measurements are been executed from a separate control room.
Given the above building facilities the following optimum arrangement resulted.
The main bank and the experiment as well as the preionisation banks have been mounted in the hall, c.f. figure P 120.
The main bank, which includes condensers, spark gaps, charging and discharging resistors and shorting breakers, forms two compact blocks with an energy density of

6,64 kWs / m^3
when considering service passages and

15,7 kWs / m^3
regarding service passages and also space for the pulse cables.

Within the bank the pulse cables run horizontaly to the precollectors. Because of the requirement of a change from a linear to a toroidal coil, a collector arrangement has to be chosen which lies asymmetrically with the height of the bank block. This results in different distances from the bank to the cable connection at the precollectors. For economical reasons only three different cable lengths have been chosen and the overshoot lengths must been arranged in the space between the bank block and the precollectors. Because of the installations norrow arrangement which was given by the building dimensions, we obtained a somewhat complicated cable loop which can be seen from figure P 124.

The Theta-Pinch preionisation with a discharge frequency of about 1 MHz will be arranged as close as possible to the load coil, c.f. figure P 120.
The bias field bank and all auxiliary equipments such as power supplies, charging disconnecting switches, trigger spark gaps, marx-generators, a fire extinguishing system and air compressors for the shorting breakers are installed in the basement room. Even here a symmetrical arrangement in two halves has been chosen as with the main bank, c.f. figure P 121.
Trigger and charging cables run vertically from the main bank to the auxiliary equipment in the basement, the overshooting length having been rolled up. A schematic graph of the geometric arrangements of the installation is shown in the figures P 122 and P 123.

4. Circuit diagram and current program

In figure P 118 a circuit diagram of one bank half is given. It contains the load, the three banks mentioned and the voltage suppression unit for the pulse cables.
Distributed inductances of the cables, of the collector system and so on appear in the form of lumped parameters; the attenuation will not be considered. Values given concern one total bank half for the connection of a linear load coil. The values for the Theta-Pinch preionisation bank have been estimated.

The main electrical data which have been compiled in figure P 119 result from the circuit diagram. This figure also shows the current waveform in the load with all three banks in operation, namely crowbarred bias field bank, Theta-pinch preionisation and main discharge. For the sake of clear representation the scales for auxiliary banks and main bank are different.

Current and voltage waveforms at several points of the installation first have been checked in the switching analog model using original cables, and later on with the aid of

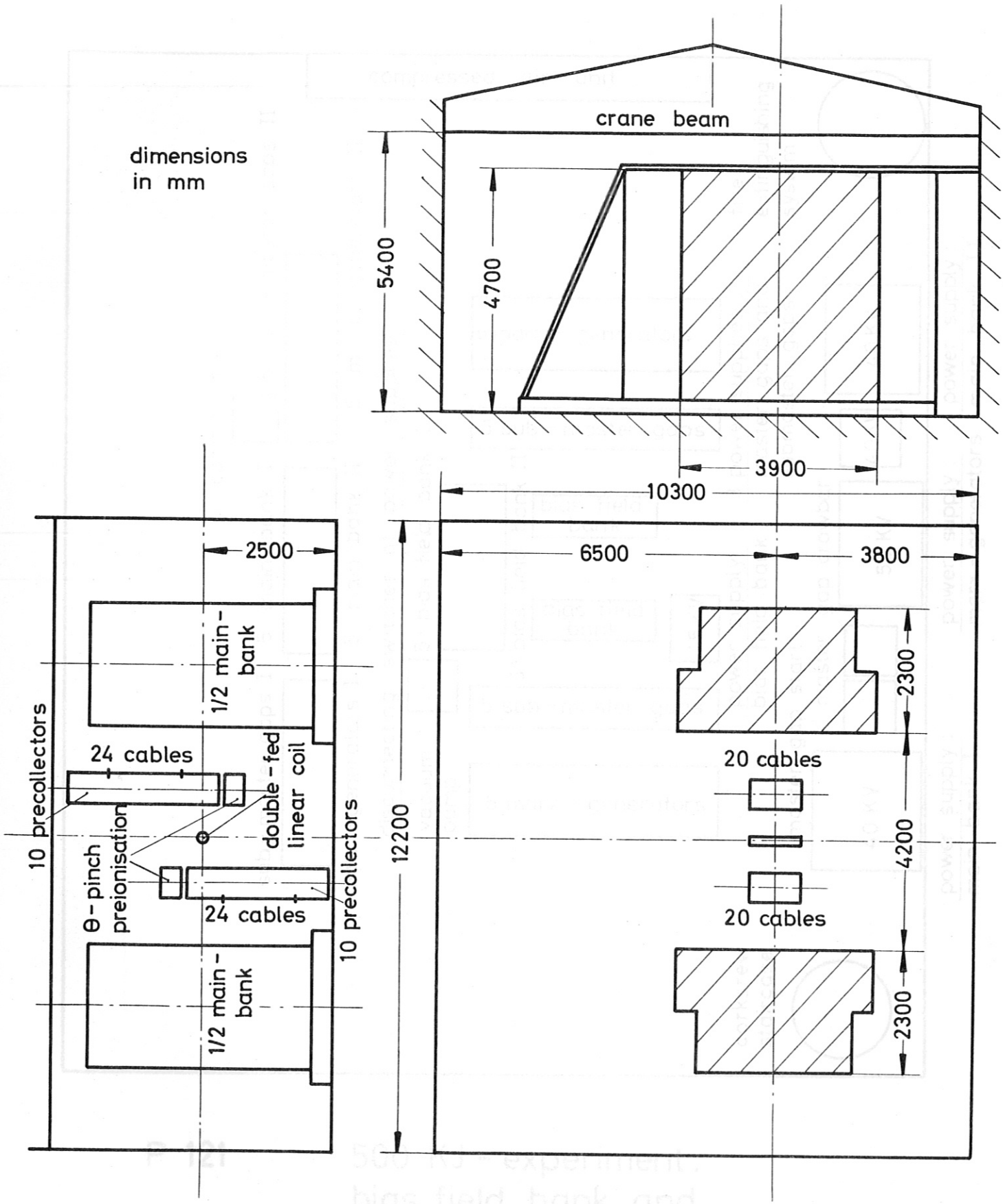

P 120

500 KJ - experiment
main bank, collector -
system and the coil.

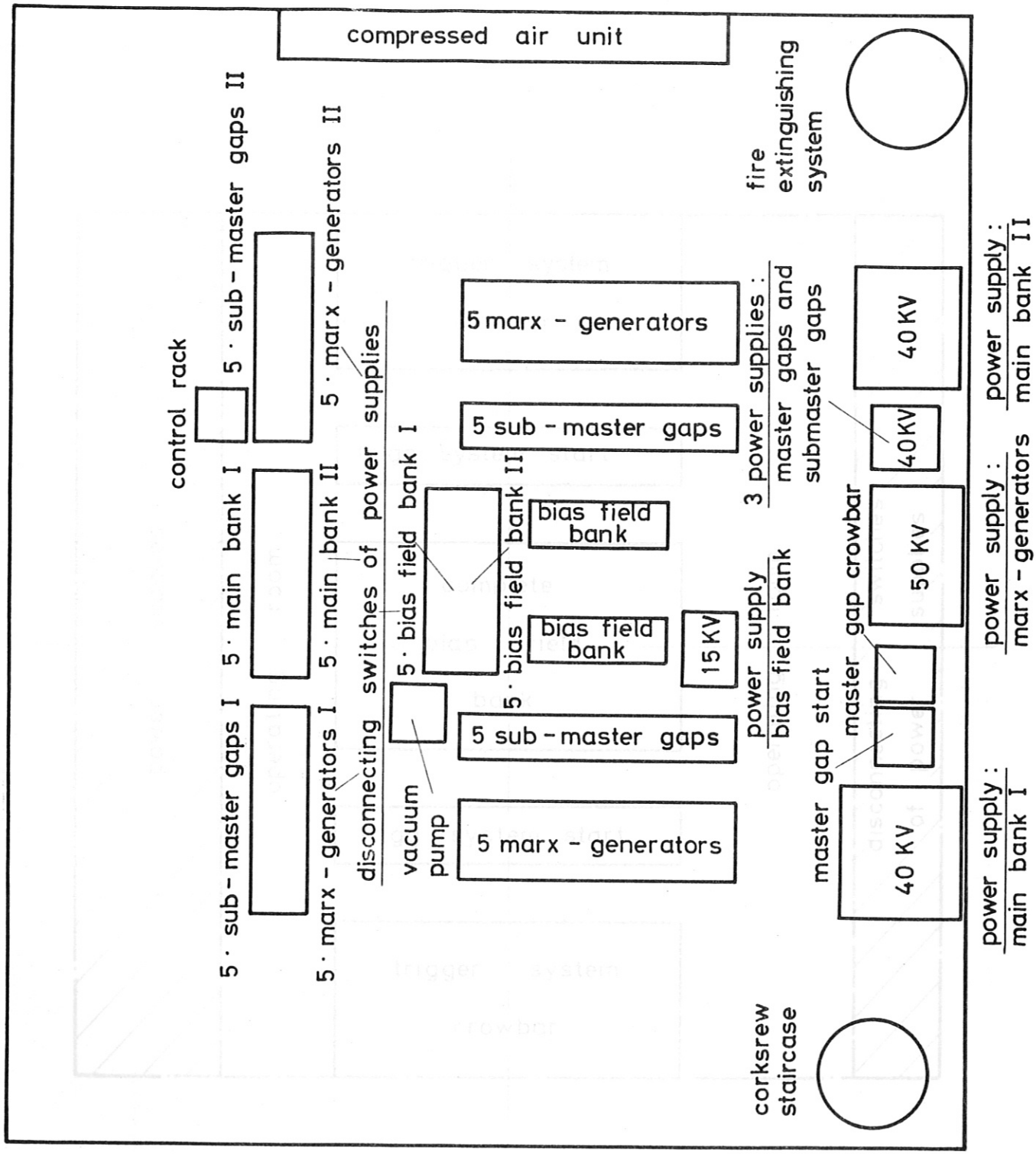

P 121

500 KJ - experiment.
bias field bank and
auxiliary units.
plan view of the basement.

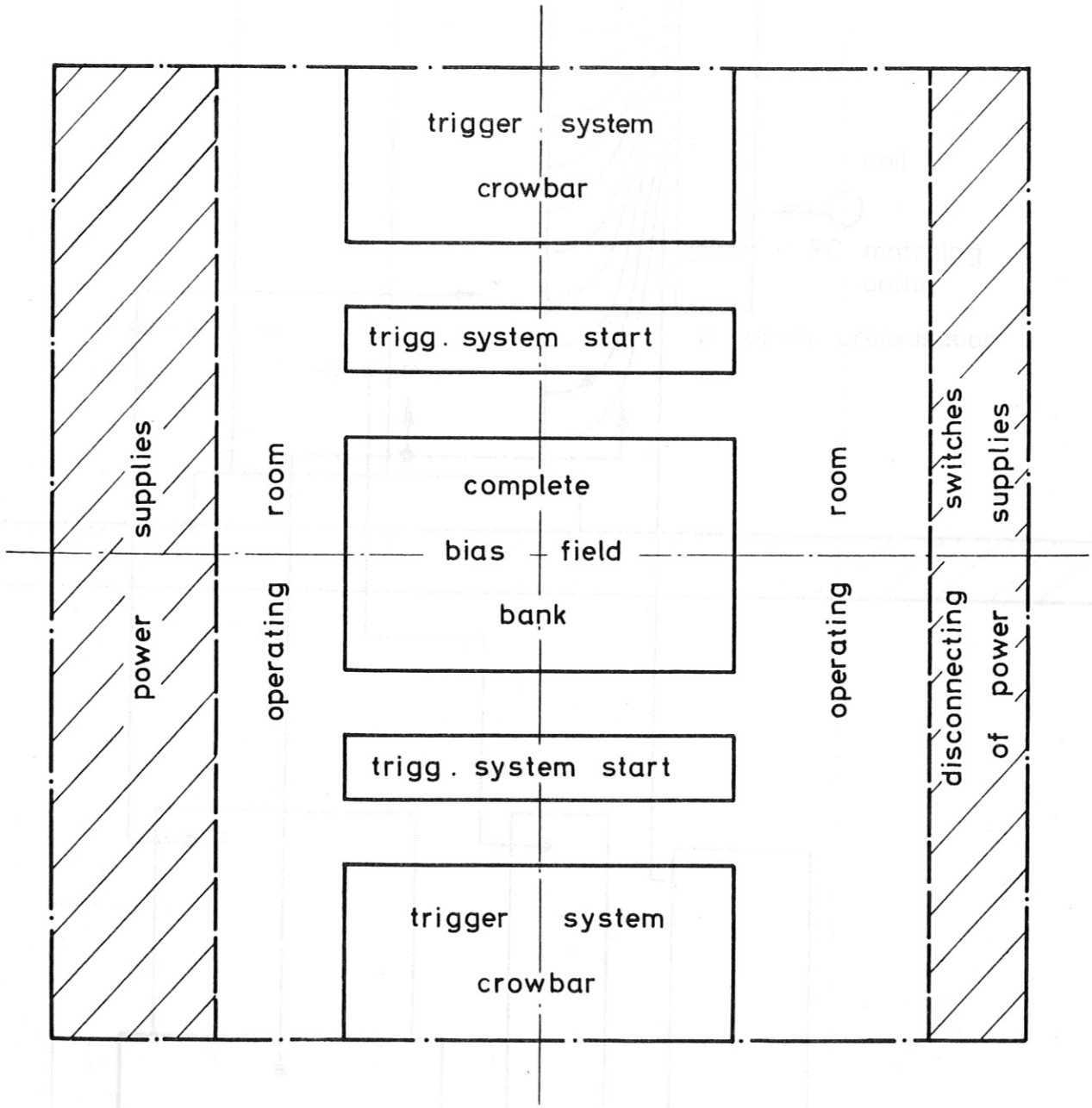

P 122 capacitor banks
structure

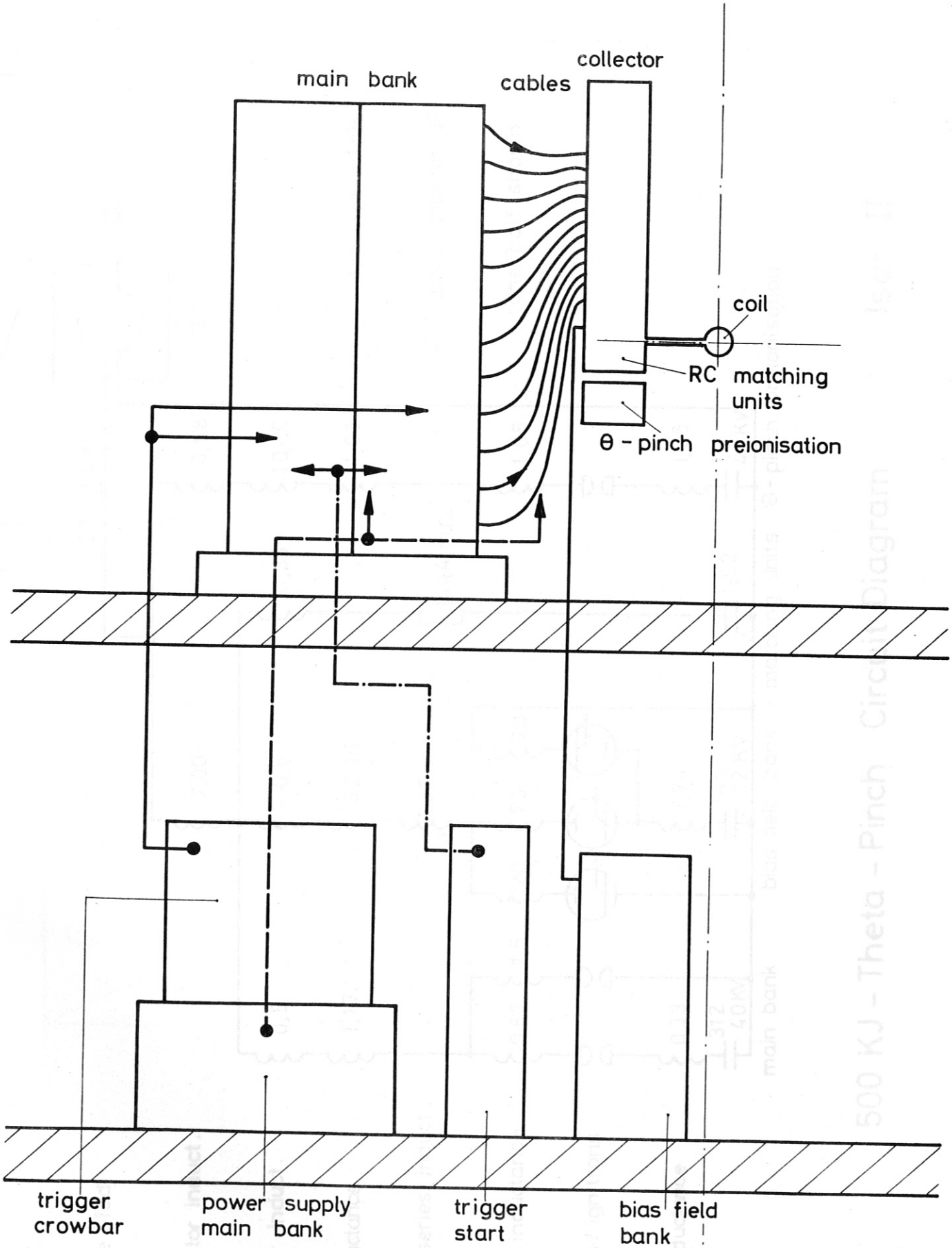

P 123 capacitor banks structure

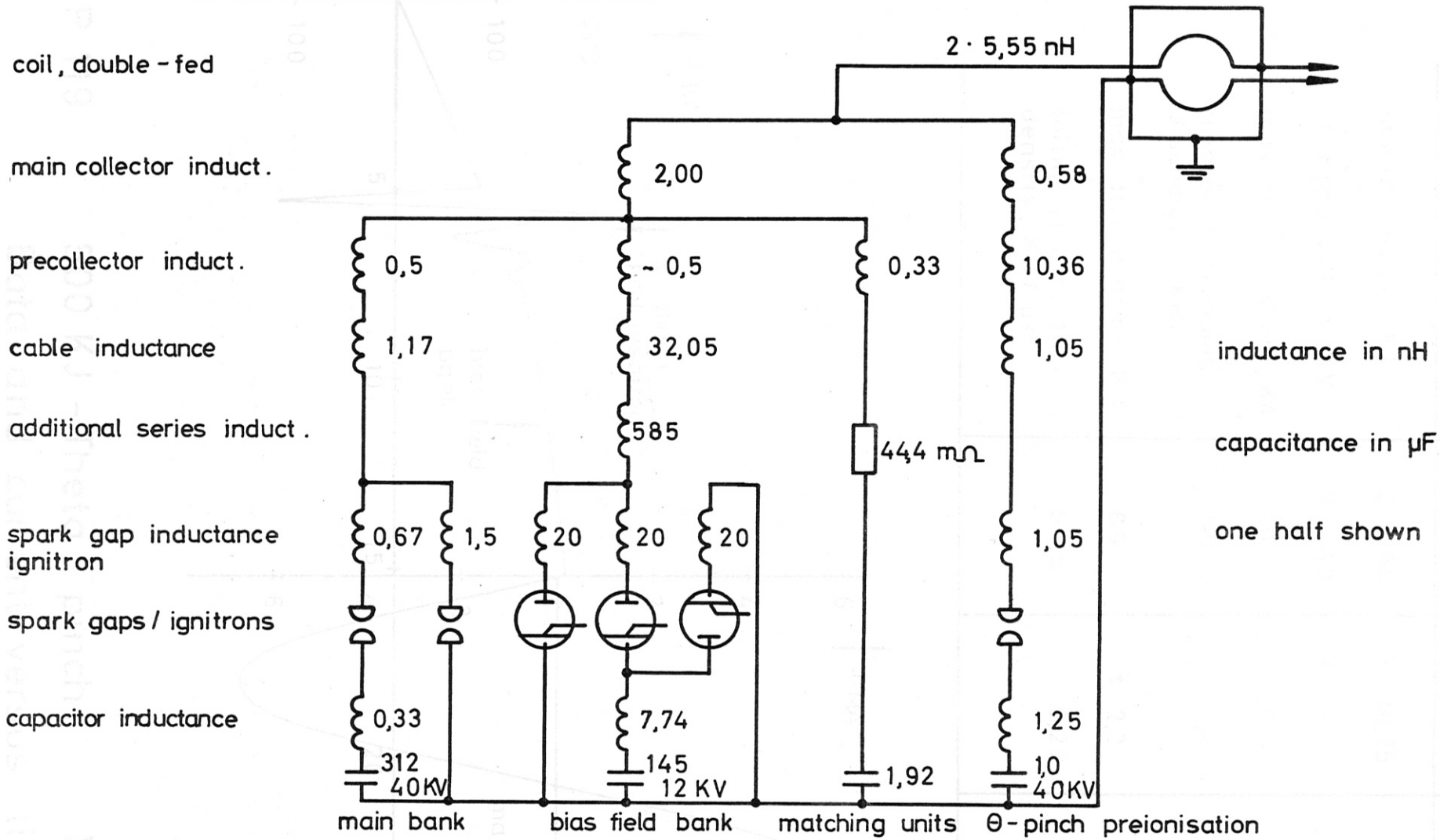

P 118 **500 KJ - Theta - Pinch Circuit Diagram** Isar II

	main bank	bias field bank	Θ - pinch preionis.
stored energy, KJ	2 · 250	2 · 10,25	2 · 0,8
charging voltage, KV	2 · 40	2 · 12	2 · 40
max. disch. current, KA	7100	180	284
frequency, swinging discharge, KHz	90	16,4	1130
max. flux density, KG	89	± 2,2	3,56
initial rise of flux density, KG / µs	50,5	0,23	25,34

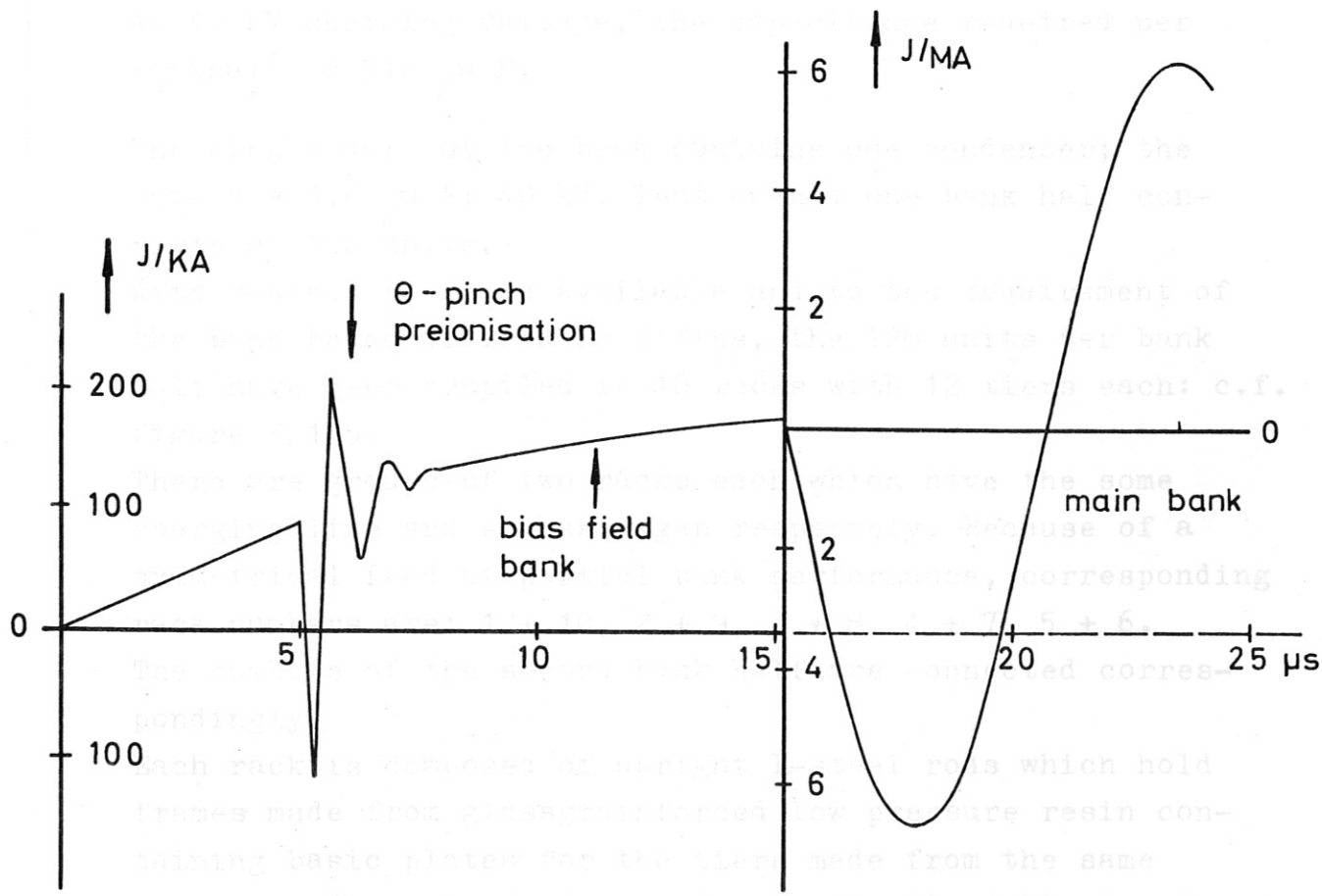

P 119 500 KJ - Theta - pinch Isar II.
Data and current versus time in the coil.

the electronic circuit analysis program (ECAP), of IBM, with a IBM computer 360/50.
The optimum values for the R.-C. suppresser units have been evaluated by measurements in the switching analog model.

5. Description of the installation and the individual components

5.1 Main bank

The capacitor bank consists of two symmetrical bank blocks with 250 kJ energy respectively. Figure P 124 shows a view of the bank halves, the collector system and the load.

At 40 kV charging voltage, the capacitance required per bankhalf is 312 /u F.

The single unit of the bank contains one condenser; the data are 2,6 /u F; 40 kV. That means: one bank half consists of 120 units.
With respect to space available and to the requirement of the bank being divided in fifths, the 120 units per bank half have been compiled in 10 racks with 12 tiers each: c.f. figure P 125.
There are groups of two racks each which have the some charging line and submastergap respectely. Because of a symmetrical feed at partial bank performance, corresponding rack numbers are: 1 + 10, 2 + 9, 3 + 8, 4 + 7, 5 + 6.
The numbers of the second bank half are connected correspondingly.
Each rack is composed of upright I-steel rods which hold frames made from glassgrainforced low pressure resin containing basic plates for the tiers made from the same material. Thus the condenser is practically fully insulated against the rods.
As already mentioned an enlargement of the bank by 60 % is possible (see dash-lined racks a to f in figure P 125)

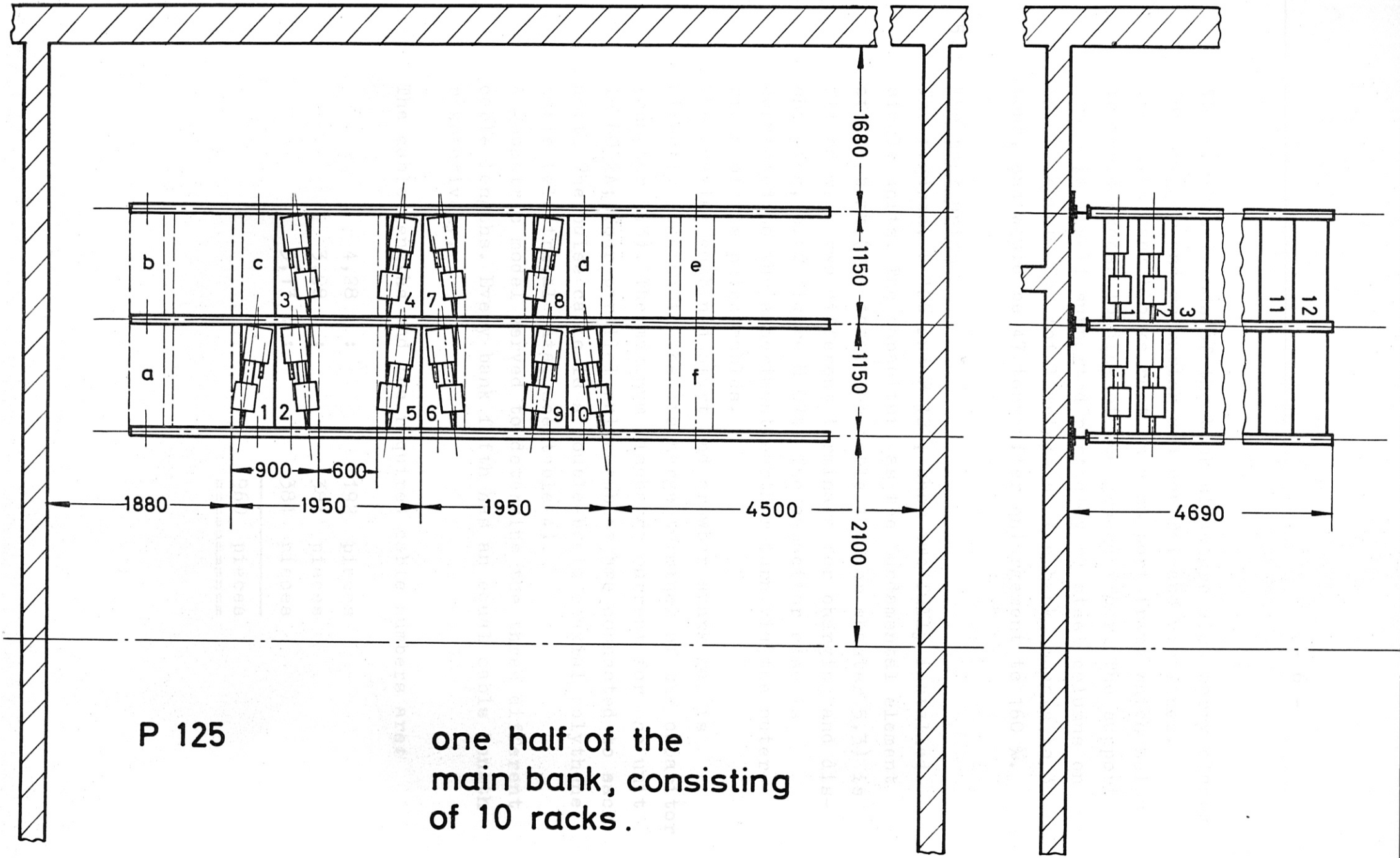

P 125

one half of the main bank, consisting of 10 racks.

The upright I-rods of the bank structure also carry clamps for trigger and measuring and control and air lines.
The total bank blocks rest on a support frame which helps to avoid excess loading of the ground floor. The support frame is itself supported partially by steel columns on the basement. The total weight of the bank amounts to 32 tons, and would be 47 tons after enlargement to 160 %.

5.2 The bank units

The figures, P 126 and P 127, show two fully installed single units. The capacitor, as the fundamental element of the bank,(for data, see table 1 after chapter 5.3) is fitted with two different terminals for charging and discharging, c.f. figure H 074. The capacitor case is connected to the experiment earth return via the outer-braid of the pulse cables.
The coaxial combined start and crowbar spark gap is directly mounted to the discharge terminal of the capacitor (chapter 5.3). The maximum discharge current for one unit is 60 kA; four parallel pulse cables are connected to each unit. The pulse cable is a double-braid coaxial polythene cable (electrical data, see table 4).
A geometric model served to determine the three different cable lengths. Every bank fifth has an equal cable length respectively.

The cable lengths and the required cable numbers are:

4,28 m :	192 pieces
3,98 m :	384 pieces
5,13 m :	384 pieces
	960 pieces

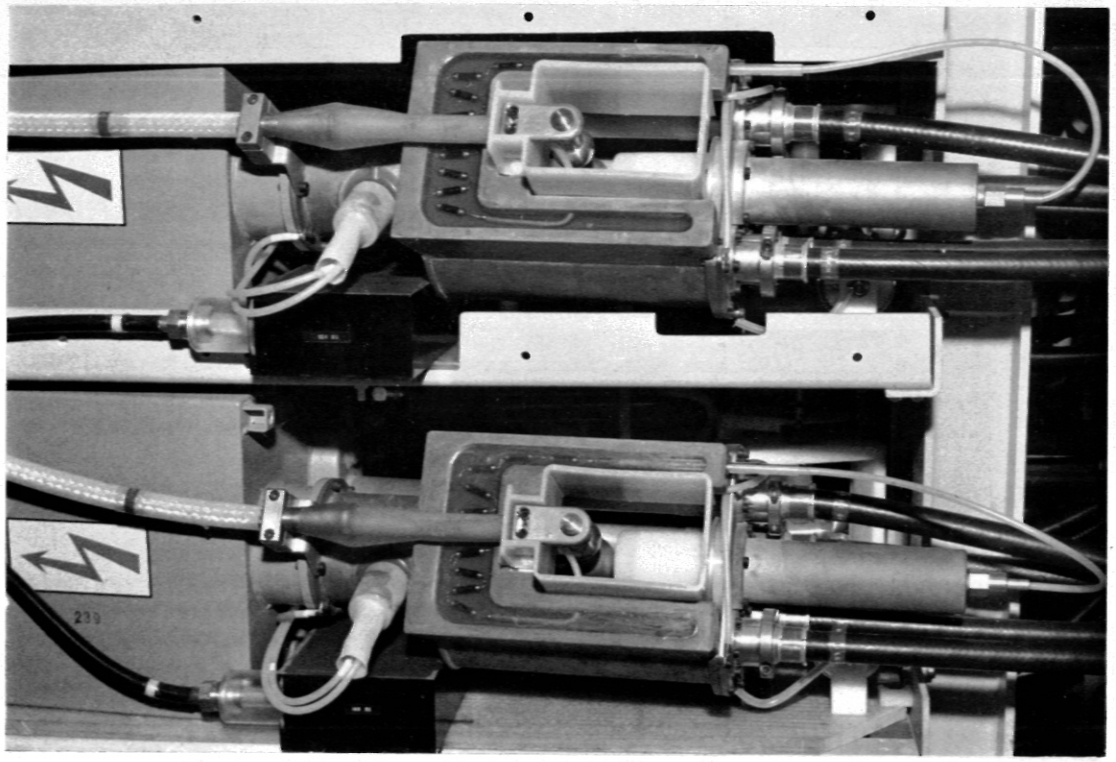

P 126 500 kJ - Theta - Pinch Isar II

Two main bank units, front side

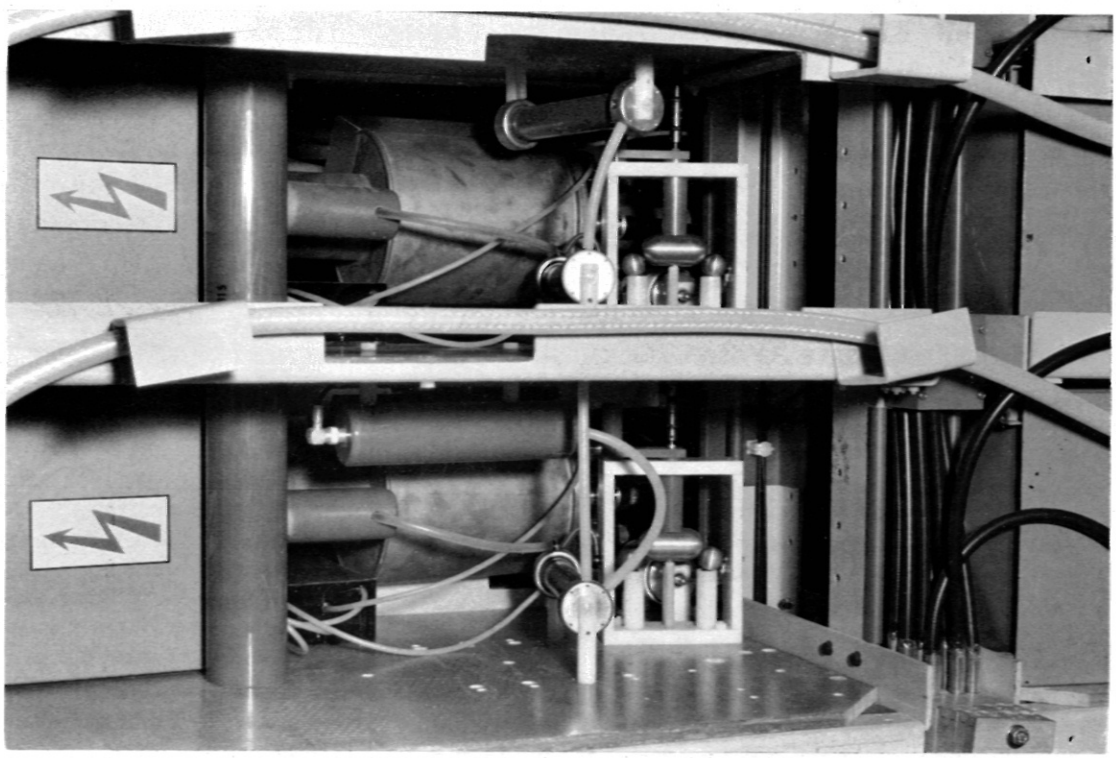

P 127

Two main bank units, rear side

The average cable length is 4,5 m. The cables are fitted with polythene terminals and are connected by detachable sliding contacts. Figure H 089 shows the contact elements for connection of inner and outer contacter of the cable (for inner contacter 22 mm Ø, for the outer 38 mm Ø).

The contact sockets have been developed in cooperation with an industrial firm, especially for the application in pulse duty. The contact socket consists of a cylindrical supporting piece which is contactet to the collector and the spark gap by means of a spring ring or a washer. The contact element consists of a large number of wire springs wich form a tulip shaped contact. The path of the high frequency current given by the geometry of the contact elements. The contact design is chosen in such a way that all current transitions have intimate connection.

Before the manufacture was started, 10 contacts of each type were tested. In these tests, with a current of 30 kA compared to a rated current of about 15 kA after 20.000 discharges, no major damage of the contacts could be discerned. Furthermore the following tests were made; 10.000 discharges were taken at 40 kA and 5.000 discharges at 50 kA without any defect. These investigations with detachable contact combinations will be persued later.

The 12 units of one rack are connected at the load side according to figure P 128. Each group of six units with a decoupling resistor of 50 kΩ is charged via a charging resistor of 200 kΩ. Four such groups of six units (=two racks; =one fifth of a bank half) are connected to one disconnecting switch in the charging equipment.

Each group of six units has also an 80 MΩ resistor, which is the upper resistor of a voltage devider and serves to measure and monitor the voltage at this group.

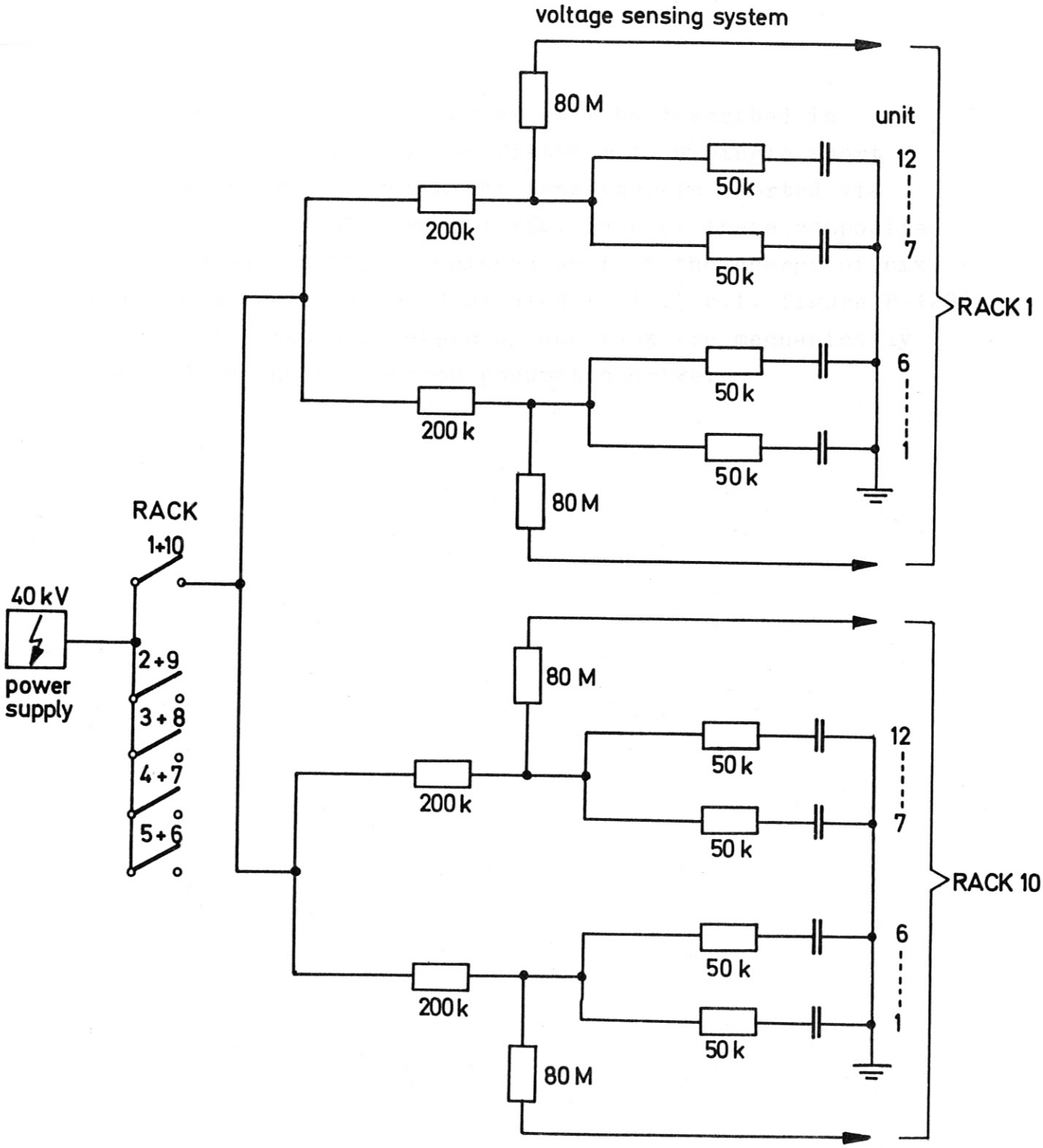

charging system P 128

The voltage monitoring device will be described in chapter 5.6. Every unit is fitted with a single short circuit breaker, by wich the capacitor is shorted via a discharging resistor of 1 kΩ. Each of these composite resitors has to be dimensioned so that the energy of six units (12 kJ) can be disipated in it.(c.f. figure P 128). The short circuit breakers of one rack are mechanically coupled and have a common pneumatic drive.

5.3. Combined Start and Crowbar Spark-Gap with Trigger-systems. (G.Klement, R.C.Kunze)

From the point of view of design of the start and crowbar switches, the condenser type with two terminals was an essential feature. One could have used a single terminal for start and crowbar spark gaps. Thus only one terminal was used and the crowbar spark gap was united with the start switch and the pulsecable connection because, in this arrangement, capacitor terminal and start switch are not loadedby the current of the crowbar switch.
No DC voltage occurs at the electrodes of the crowbar switch, and the resistance and inductance of the crowbar branch becames lower. The condenser used, a coaxial terminal and a charging terminal (insulator embedded in epoxy resin) can be seen in figure H 074. The data of energy storage capacitor will be shown table 1.

The start switch.

A correct switching function of the start spark gap, when operating in parallel with a large number of other spark gaps, requires a jitter time which is smaller than 38 nsec in this case. That is double the delay time of the shortest load cable.
With respect to the operating range desired, the four electrode cascade gap was chosen which gave small dimensions in a coaxial arrangement as well as low inductance. The method of operation of the four electrode spark gap has often been treated in previous papers (1)(2)(3) and therefore will not be described here at length.
The common electrode, whose potential lies between the charging voltage of the capacitor and earth potential, c.f. figure H 075, is shifted by

a trigger pulse to a potential opposite to the charging potential. The over voltage effects the breakdown of the gap A - B and brings the common electrode to the charging potential of the capacitor or higher (swinging cascade); consequently the gap B - C also will break down.

In the start switch used here, the relation between both breakdown voltages is $\frac{A - B}{B - C} = \frac{3}{2}$; that is, the common electrode lies stationary on 2/5 of the charging voltage. The 40 kV and 20 kV charging voltages correspond to 72 % and 36 % respectively of the breakdown voltage U_D which is 56 kV.

Figure H 076 shows the static breakdown voltage between the common and the outer elektrode (electrode distance A - B and B - C) .

In the common electrode there is a small spark gap as a light source, which essentially in fluences the performance of the cascade. As can be seen from figure H 077 , the jitter and partially the operating range of the switch depend on the adjustment of this light source.

For the arrangement according to figure H 075, the delay of the spark gap is given by figure H 078.

The oscillogram H 080 shows the voltage wave form at the cable termination. This photograph has been taken from a series of jitter measurements. Also figure H 079 shows the voltage waveform at the common electrode.

The static and dynamic matching of the spark gap, optimised according to jitter and recurrent voltage dependence, had to be concentrated in matching units. These units, in which the elements have been embedded in " Sibit", are to be seen in figure P 126 below the coaxial start spark gap.

Evaluating the oscillograms H 081 and H 082, one finds a maximum current per unit of 62 kA for 1oo kHz and the inductance of one unit to be 980 nH.

The data of the start switch in detail are summarized in table 2.

The crowbar switch.

A crowbar switch, lieing in parallel with capacitor and start switch, must be able to hold the full voltage (discharge voltage with supperimposed cable reflexions), but on the other hand has to switch at practically no voltage. The tolerable jitter of such a switch depends in the main part on the discharge frequency of the installation. At low discharge frequencies, a comparatively large jitter can be tolerated. The fundamental requirement for a switch for this performance is

$$R_{Cr} < \omega_{Cr} L_{K+ SFS} < \omega L_V$$

As the design of the energy storage system tends to minimise the internal inductance of the capacitor bank, and as crowbar ripple should be as low as possible, the inductance of the crowbar gap must also be as low as possible. From the different types at hand a simple two electrode crowbar spark gap triggered by overvolting was chosen (4)(5)(6)(7) .
With the nomenclature of the circuit diagram, H 075, the performance can be described as follows. In order to breakdown the gap between the electrodes C and F, the required voltage is generated at a given ferrite inductance. This is achieved by a triggerpulse applied to the pulse sharpening spark gap E-F , which premagnetises the ferrite rings at the same time. Without premagnetisation, the voltage occuring at electrode F is considerable smaller, according to the relation,

$$\int_0^{t_s} u\, dt = -\phi_v - \phi_s > \phi_o - \phi_s$$

After the gap C-F has been closed and the ferrites saturated, only the air inductance of the assembly is efficient.
The trigger pulse waveform at the pulse sharpening electrode is according to figure H 083 and the voltage

at the ferrite decoupled electrode has been measured according to figure H 084. Figure H 086 gives the waveform of the load current. The decay time constant L / R, for the crowbar discharge as T = 80 µsec. , from a measurement at a test rig containing 6 units with one half precollector. Therefore, the calculated resistance R of the crowbar spark gap is 7 m Ω .
The currents in the three branches of the crowbar circuitry are shown in figure H 090.
The measured inductance of the coaxial crowbar switch connected between the cable terminals amounts to 180 nH.
The crowbar ripple is given by the approximation,

$$w \approx \frac{L_{Cr}}{L_v} \quad 100\ \% = 21\ \%$$

The oscillogram H 085 shows the current in the load, which is given a ripple of

$$w = \frac{J_1 - J_2}{J_1 + J_2} \quad 100\ \% = 25\ \%$$

Deviation between the two values results from the higher discharge frequency in the rig with 6 units.
Correcting to 100 kHz, the same ripple of 21 % results:

$$w_{f_1} = w_{f_2} \frac{f_1^2\ 4\ \pi^2\ C - L_{K+SFS}}{f_2^2\ 4\ \pi^2\ C - L_{K+SFS}}$$

For the electrode material of the cascade and crowbar spark gap copper was chosen, since it is little eroded. Furthermore, copper is useful because it gives rise to only slight vapor-deposition on the insulating parts. The rough surface of the electrodes after several discharges will not be very dangerous for an atmospheric pressure spark gap. After 10 000 discharges at 100 kHz, $\hat{I}$ = 62 kAand 30 sec. duty cycles, the erosion at the common electrode was minimal. [(2) cf. photograph of main and trigger electrodes after 1o 000 discharges.]

Constructive design.

As indicated in figure H 087, the start and the crowbar spark gaps are coaxially arranged in the same case. Epoxy resin was used as the insulating material for both gaps, as well as for the insulation overlap with the capacitor terminal. The hot start spark gap electrode is screwed on to the capacitor terminal bolt, where as the common electrode, with the pre spark gap, is embedded in epoxy resin and can be adjusted externally. Two calottes, as common electrode C for the start and crowbar switches, are fixed on the connecting plate with the contact sockets for the parallel pulse cables.
The crowbar spark gap lies in the inner region between the cable terminals and forms, together with these terminals a coaxial system. (cf. figure H 088)
Because of the small distance between the arc of the crowbar spark gap and the polythene terminals of the pulse cables the terminals have been fitted with an additional PE - protection sheet, which can be easily replaced.
Through the cooperation of the Institut für Plasmaphysik and the cable makers, the cable terminals shown in figure H 089 has been developed. The cable termination consists of PE as the cable insulator. An end- electrode from conducting PE, at the end of the outer braid, reduces the field gradient on the PE -insulation surface, as well as in the internal region. Inner and outer braids are connected to the contact parts on the terminal by magnetically fixed shrinking rings.

Trigger system for start spark gaps.

The trigger pulse for the start spark gaps is generated by a 10 m long coaxial cable, (Z = 70 Ω), which is charged to 30 kV and shorted by a submaster spark gap at one end. Because the division of the bank given, each submaster gap (8) feeds 24 cables, thus 10 submaster gaps in total are required. These spark gaps are triggered by a common master spark gap. The trigger system of the submaster gaps is the same as the system for the start spark gaps, the charging voltage of the 10 m long cables being only 20 kV. The master spark gap, which feeds 10 cables, is insulated from the 15 kV trigger generator (9) by a pulse transformer. In figure H 091, the intire trigger system is represented.
The trigger spark gaps according to figure H 092 respond in their function and design to the start spark gap already described. In the life test of one master spark gap on HNO_3 deposition occured on the copper electrodes and on the insulation, which are disturbed the switching function. By means of additional bores in both main electrodes the spark gap is vented and prevents the above deposition. The submaster spark gaps operated at 30 kV charging voltage are adjusted to 40 kV static breakdown voltage. The master spark gap operates at 20 kV charging voltage and is adjusted at 30 kV static breakdown voltage.

Trigger system for the crowbar spark gaps.

A two stage Marx Generator with a capacitance of 2 x 1,1 µF and 12m long coaxial cables gives a 100 kV pulse for triggering the crowbar spark gaps. The charging voltage U = 35 kV of each stage, doubled by series connection, produces a theoretical pulse voltage of 140 kV at the opened terminal of the cable (pulse sharpening electrode of the crowbar switch). The pulse voltage rise time essentially is given by L / R . For the actual design, that is 24 cables connected per Marx Generator , the values are $R = 2\,\Omega$, $L \sim 0{,}6\,\mu H$. This means a rise time of about $t \sim 300$ nsec. The Marx Generator in the lower stage is triggered by a length-wise triggered three electrode spark gap. The second two electrode spark gap of the upper stage is triggered by overvoltage. According to the arrangement for the start spark gap trigger system, the 10 Marx Generators are triggered by a master spark gap and a 15 kV trigger generator. Figure H 093 shows the circuit diagram of the crowbar spark gap trigger system and in figure H 094 the installed Marx Generators of one bank half are illustrated.

Figure H 094 is a photograph of the crowbar trigger cable terminal for the side of the crowbar switch. This terminal has to be conical for perculiar reasons to this switch. At this point a maximum voltage occurs, equal to the breakdown voltage of the pulse sharpening spark gap. In the same figure the cylindrical terminal for Marx Generator connection is shown.

Table 1

Energy Storage Capacitor (10)

Capacitance	C	= 2,6 μF
Charging voltage	U	= 40 kV
Energy	W	= 2,o5 kJ
Inductance (one coaxial terminal)	L	= 40 nH
Output resistance	R	= 16 mΩ
Resonance frequency	f	= 500 kHz
Life quarantee f=100 KHz, $\hat{I}$=62 kA	s	= 25000 discharges

Table 2

Start spark gap.

Main electrode diameter	d	= 50 mm Ø
Common electrode diameter	d	= 23 mm Ø

Electrode distances

A - C = 22 mm	U_{DC}	= 56 kV
A - B = 14 mm	U_{DC}	= 33 kV
B - C = 8,5mm	U_{DC}	= 22 kV
B - D = 1 mm	U_{DC}	= 3 kV
Inductance	L	= 4o nH
Resistance	R	= 8 mΩ
Working range	U	= 2o...4o kV
Jitter	Δt	$<\pm$ 1o nsec
Delay	t	=12o..2oo nsec
$\int$idt swinging discharges	Q	= 1,5 Asec
Inductance of cable terminal	L	= 4o nH

Table 3

Crowbar spark gap

Diameter of the electrode C	d =	5o mm ø
Diameter of the electrode F	d =	5o mm ø
Diameter of the electrode E	d =	35 mm ø
Electrode distance ..... C - F	=	2o mm
Electrode distance ..... E - F	=	35 mm
Resistance	R =	7 m Ω
Inductance	L =	18o nH
Ferrite inductance	L_{Fe} =	21o /uH
Premagnetisation resistance	R =	2 kΩ

Crowbar discharging

Ripple (f = 1oo kHz)	w =	21 %
$\int$ idt.....	Q =	4,6 Asec
Decay time constant L/R	T =	8o /usec

Table 4

Coaxial pulse cable (type 2YC2YC2Y 24x8xo,3, 24x1oxo,3)

DC resistance of both conductors	R =	1,5 m Ω /m
Capacitance	C =	345 pF/m
Inductance	L =	125 nH/m
Impedance	Z =	19 Ω

Table 5

Crowbar trigger cable (type 6,4/18,5)

Capacitance	C =	145 pF/m
Inductance	L =	297 nH/m
Impedance	Z =	45 Ω

Table 6

Start trigger cable (type 2,o L/ 12)

Capacitance	C =	72 pF/m
Inductance	L =	332 nH/m
Impedance	Z =	7o Ω

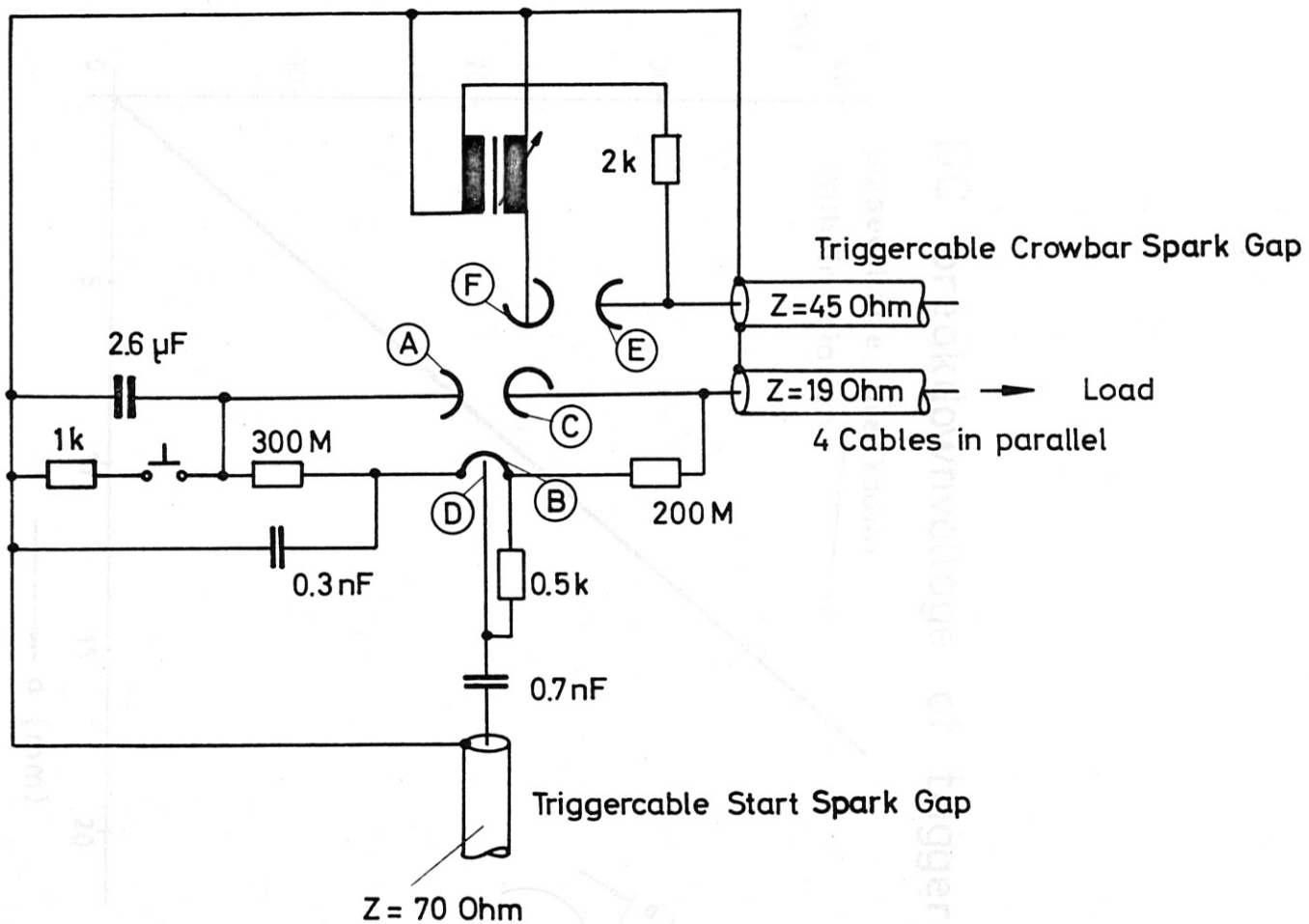

H 075 Circuit diagram of the Start and Crowbar Sparkgap

DC breakdownvoltage of triggerelectrode

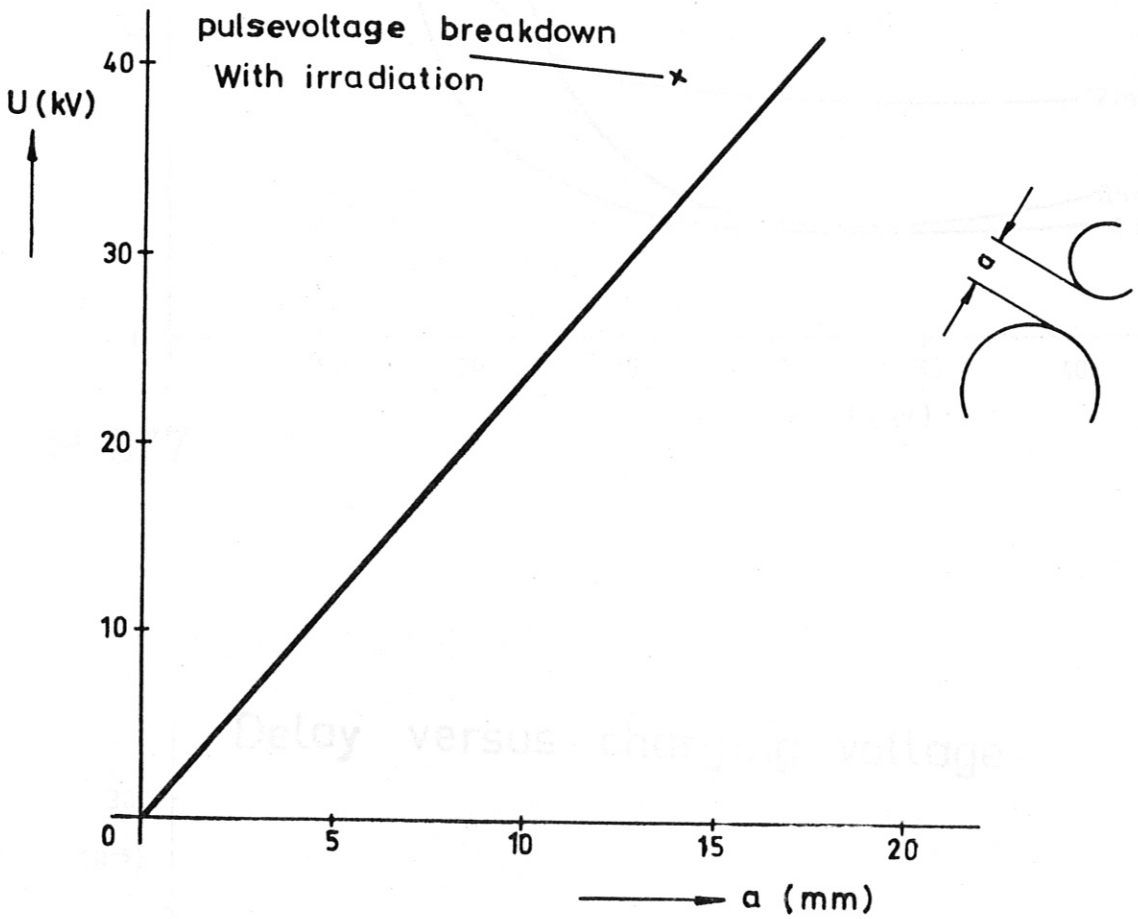

H 076

Jitter versus charging voltage

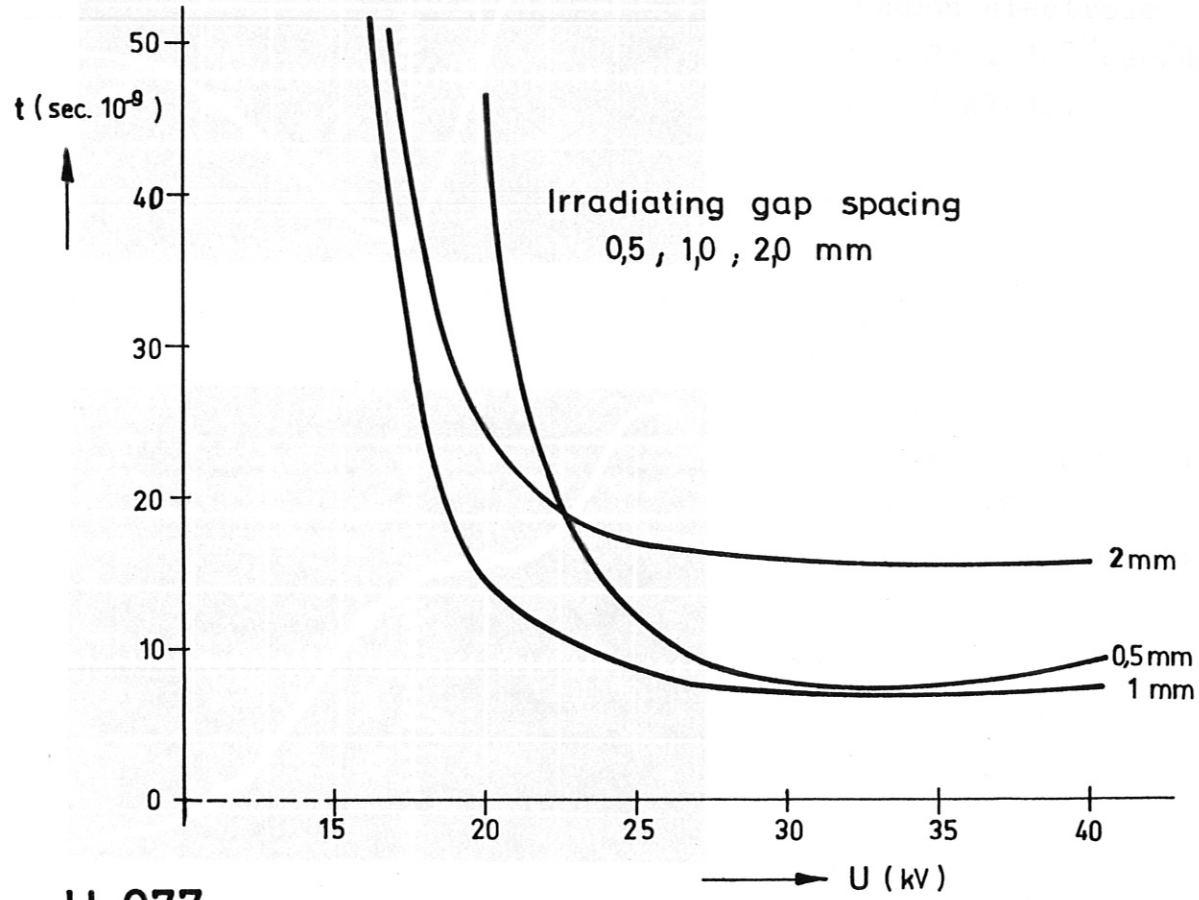

H 077

Delay versus charging voltage

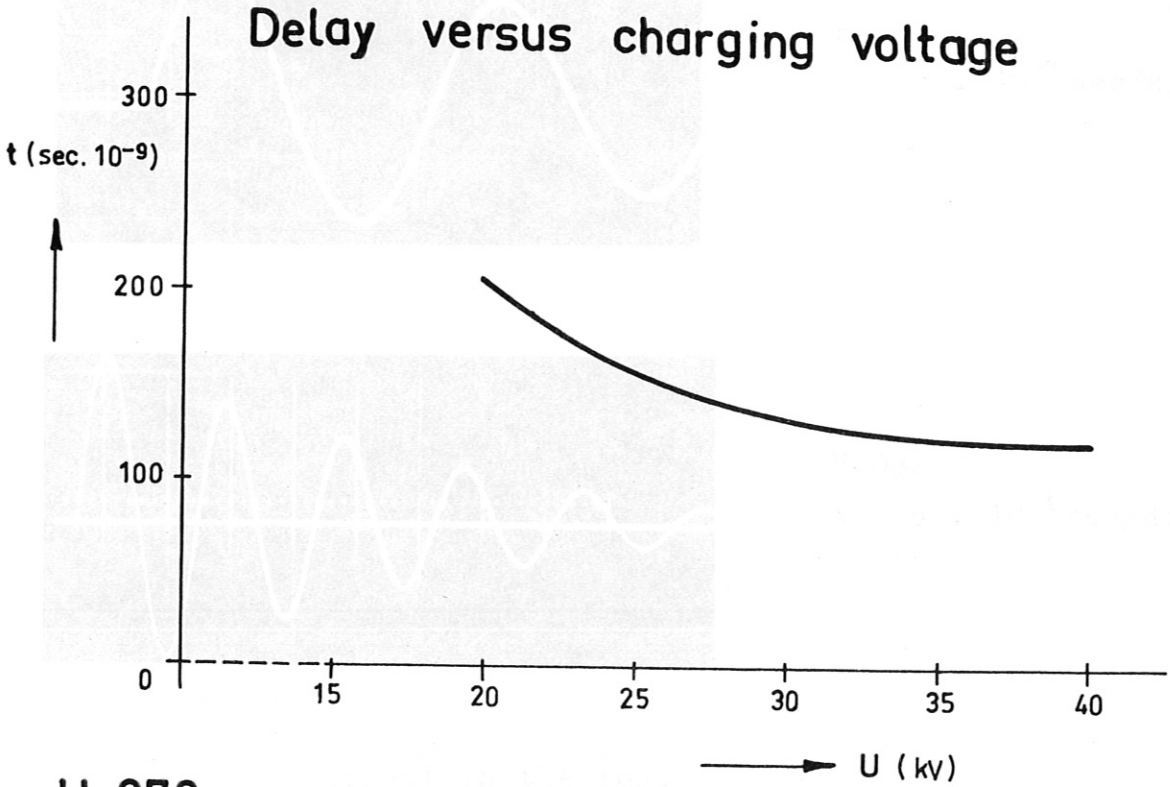

H 078

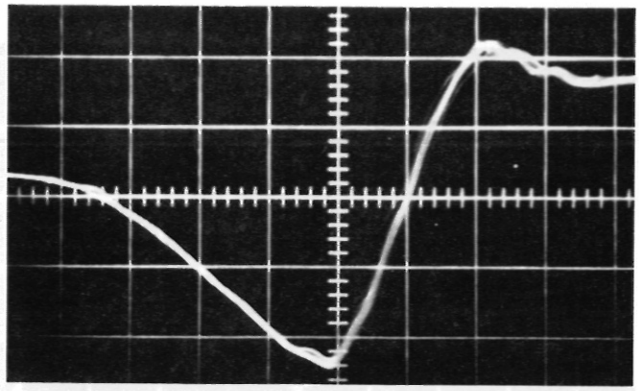

H 079
common electrode
$t = 20 \cdot 10^{-9}$ sec/div
$u = 7$ kV/div

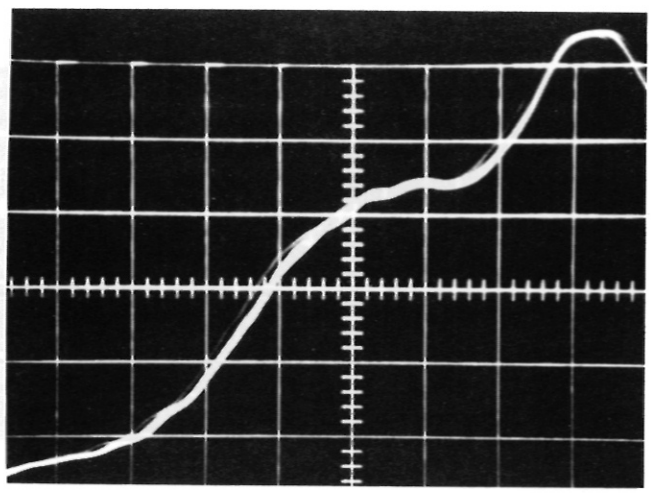

H 080
output of spark gap
$u = 10$ kV/div
$t = 20 \cdot 10^{-9}$ sec/div

voltage waveforms

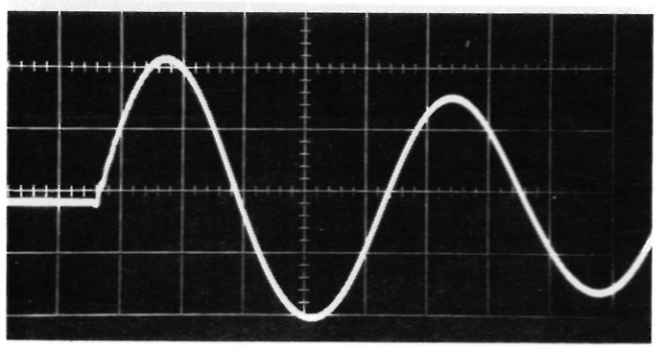

H 081
$t = 2 \cdot 10^{-6}$ sec/div

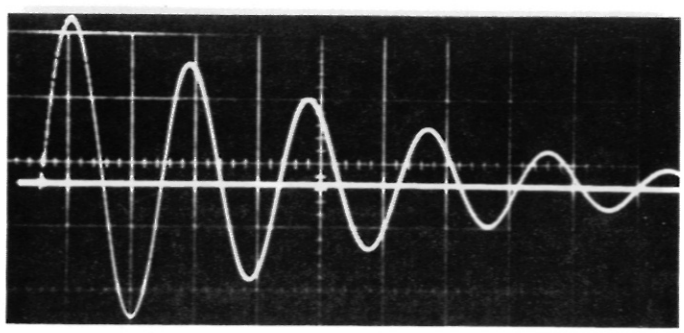

H 082
$t = 5 \cdot 10^{-6}$ sec/div

current in the load

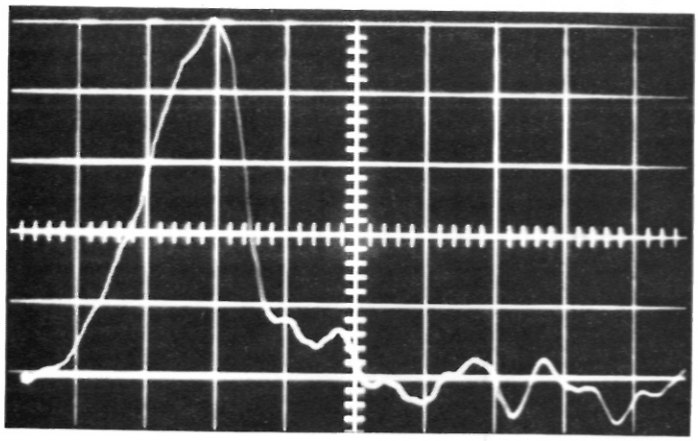

H 083
voltage waveform at
pulse sharpening
electrode E
u = 20 kV/div
t = 100 . 10^{-9}sec/div

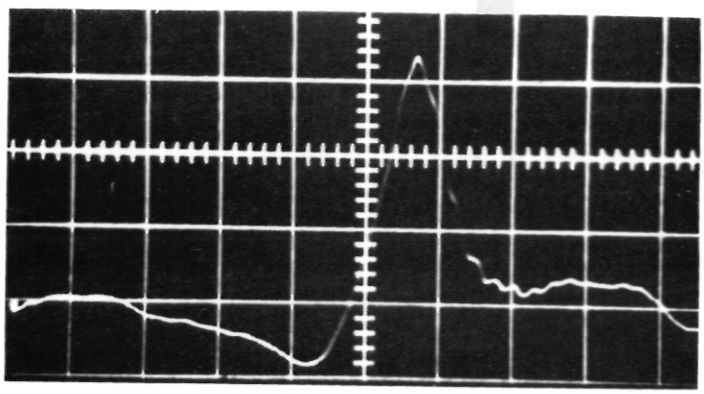

H 084
voltage waveform at
ferrite decoupled
electrode F
u = 23 kV/div
t = 100 . 10^{-9}sec/div

trigger pulse for the spark gap

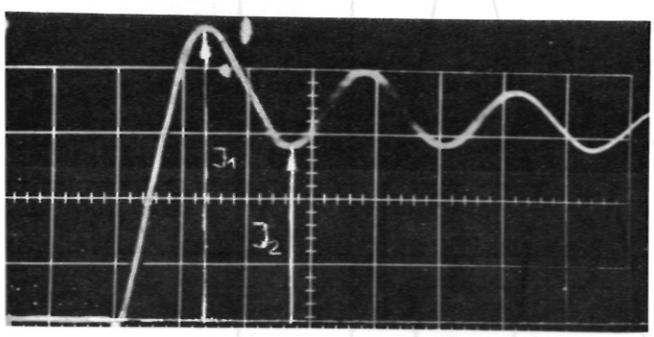

H 085
current in the load
t = 2 . 10^{-6}sec/div

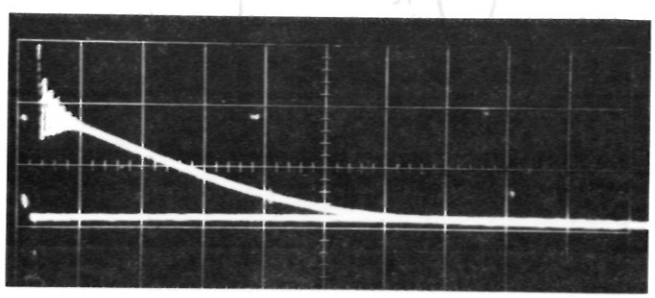

H 086
current in the load
t = 50 . 10^{-6}sec/div

crowbar discharges

Circuit diagram

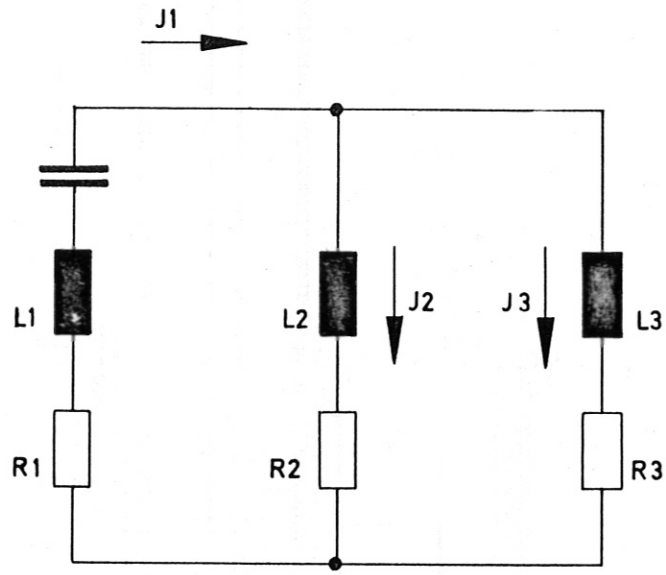

Currentwaveforms

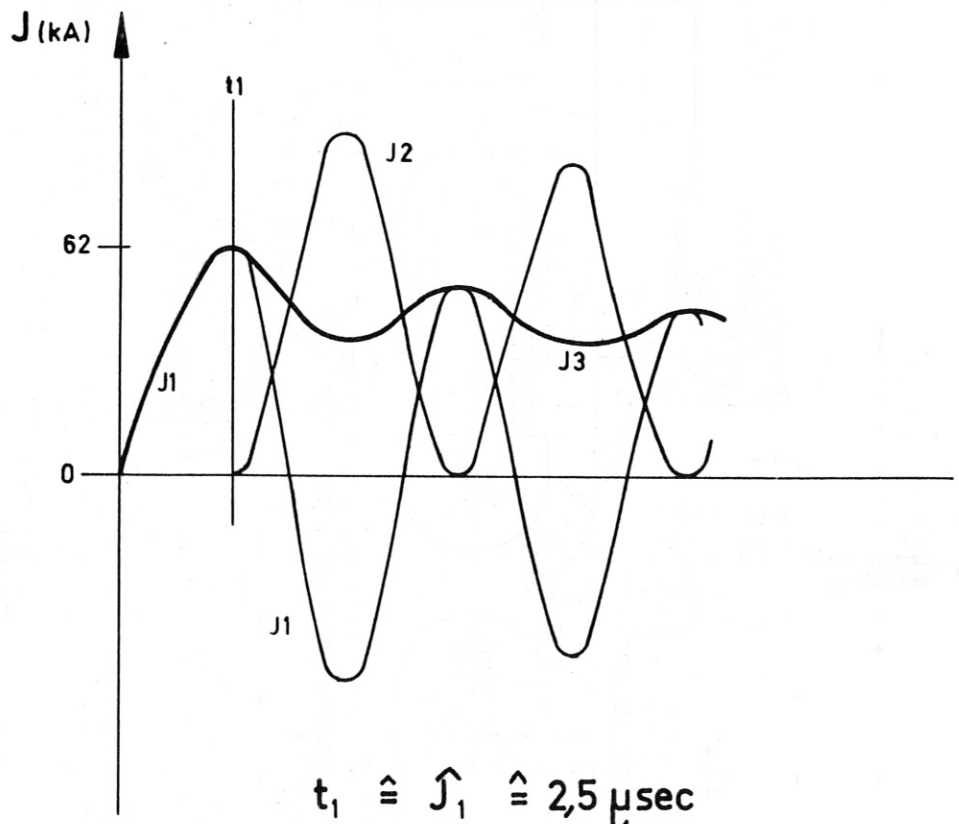

$t_1 \mathrel{\hat{=}} \hat{J}_{1\,max} \mathrel{\hat{=}} 2{,}5\ \mu sec$

H 090

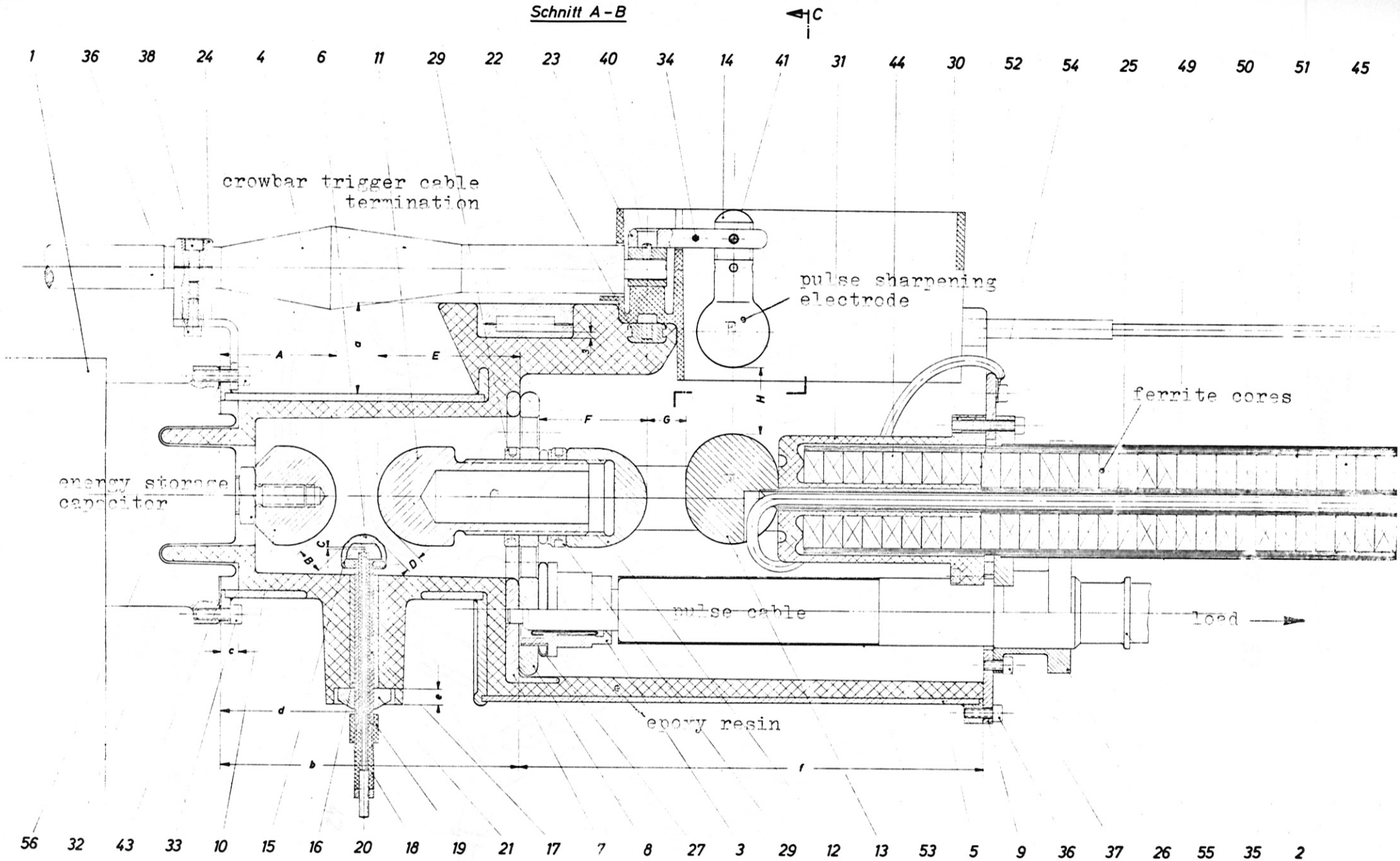

combined main and crowbar spark gap
with coaxial capacitor termination

Ho87

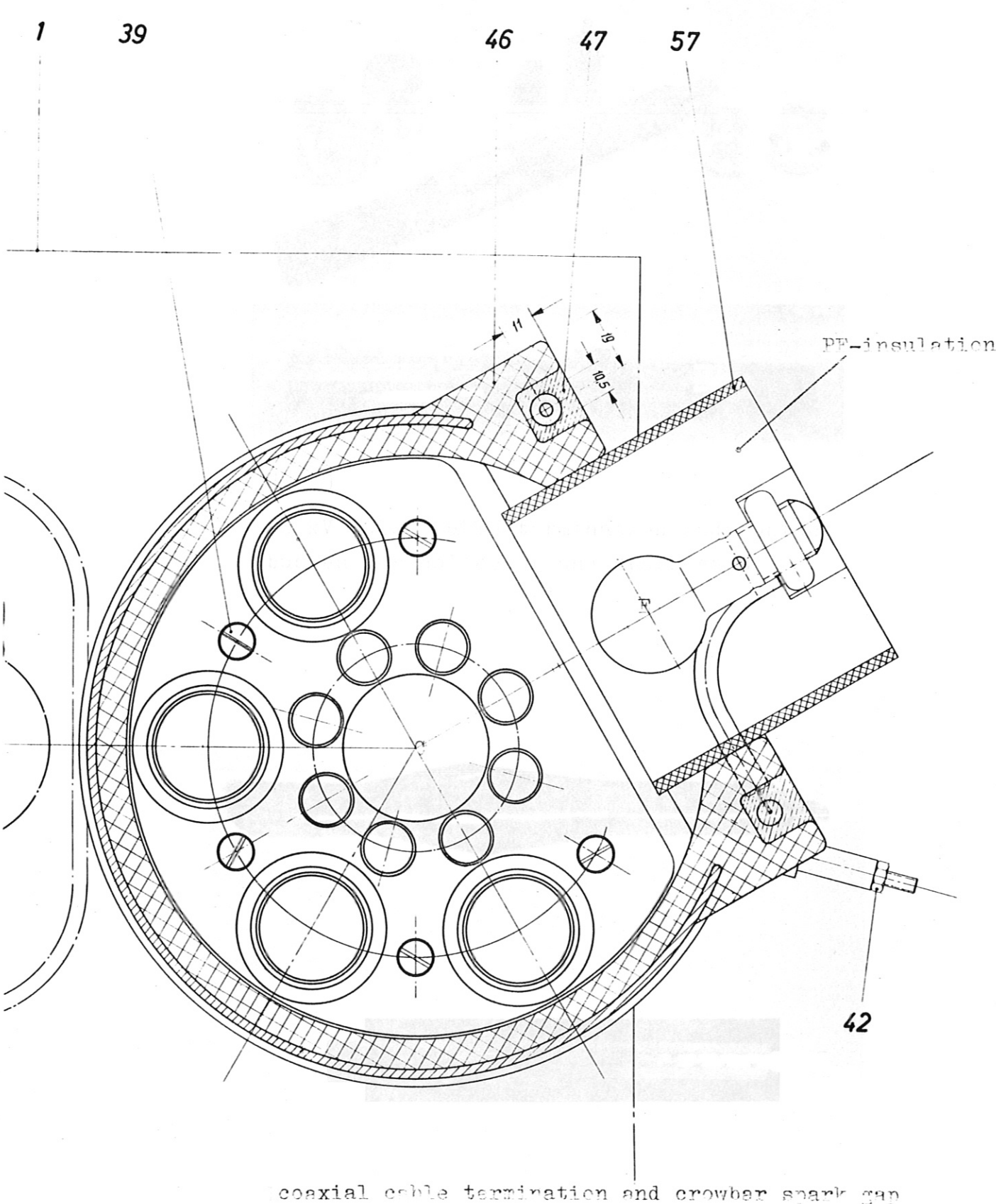

coaxial cable termination and crowbar spark gap
with pulse sharpening electrode

H 089

40 kV pulse cable termination and contact bushes for collector and spark gaps

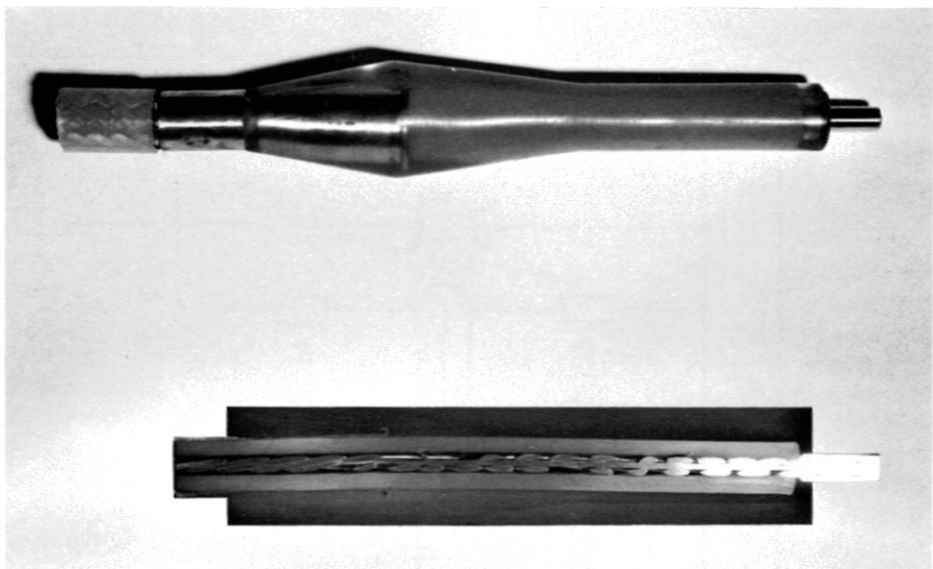

H 095

crowbar trigger cable termination moulded in epoxy resin

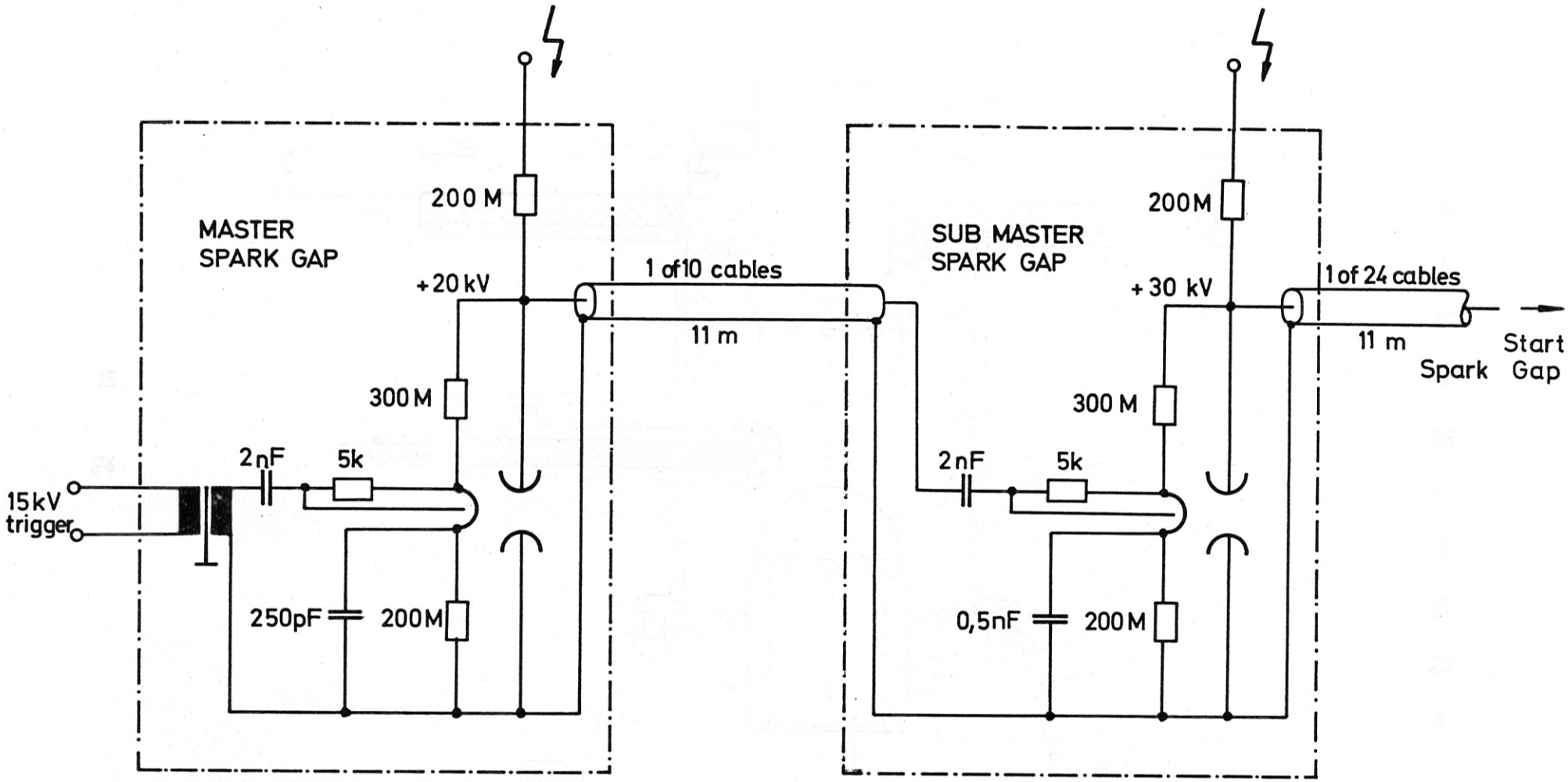

H 091 Triggercircuit of the Swinging Cascade Sparkgap

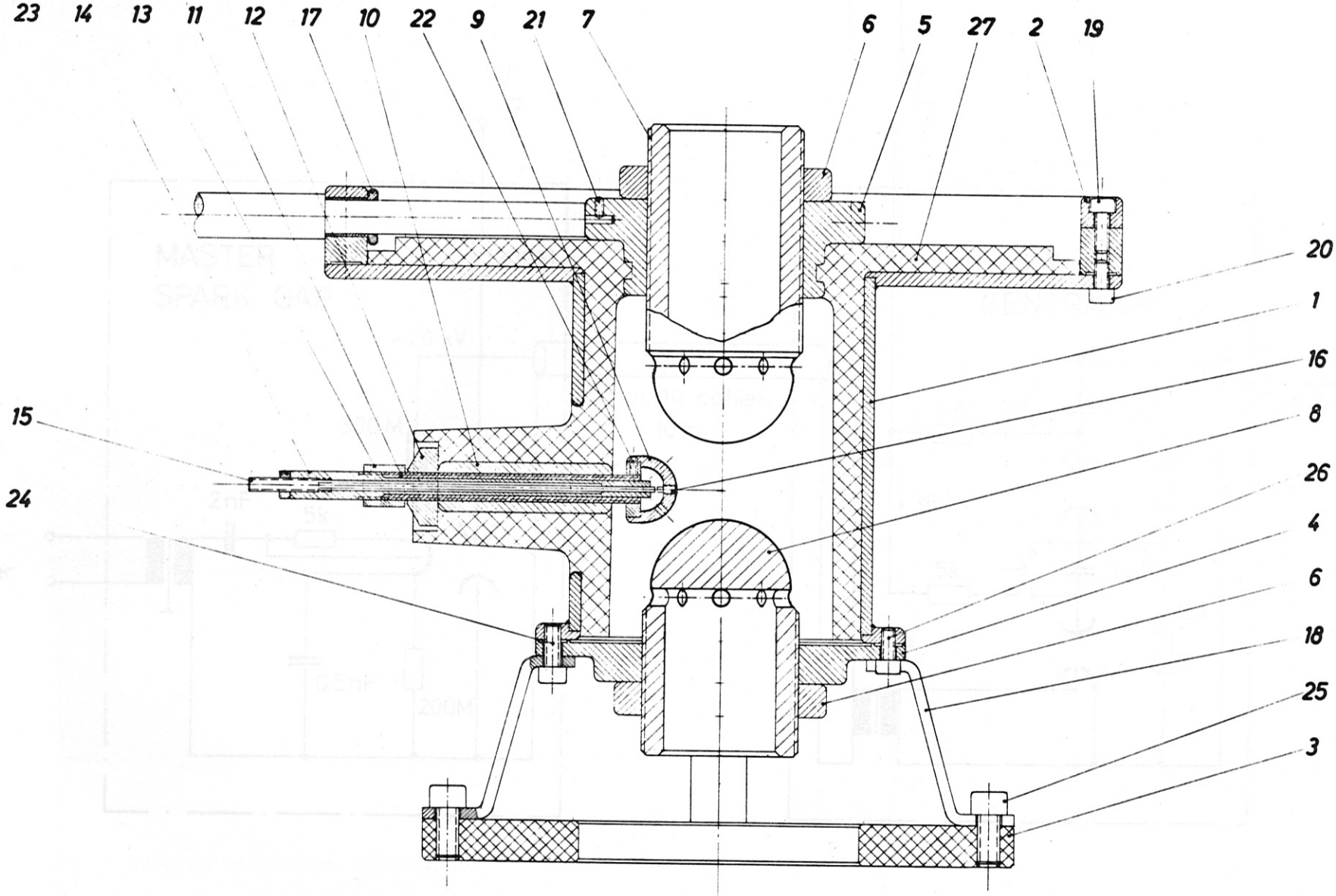

master spark gap Ho92

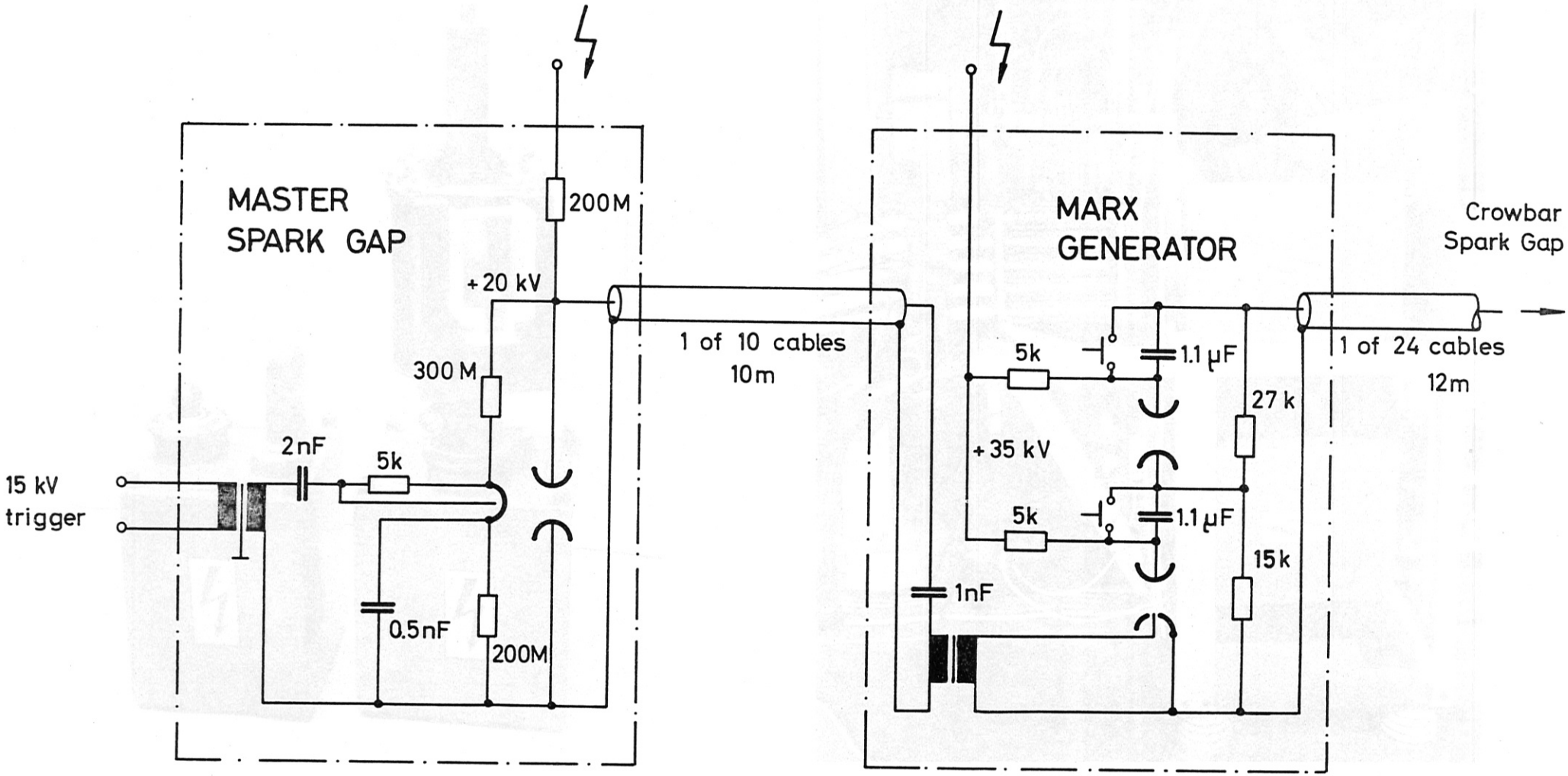

H 093 Triggercircuit of the Crowbar Sparkgap

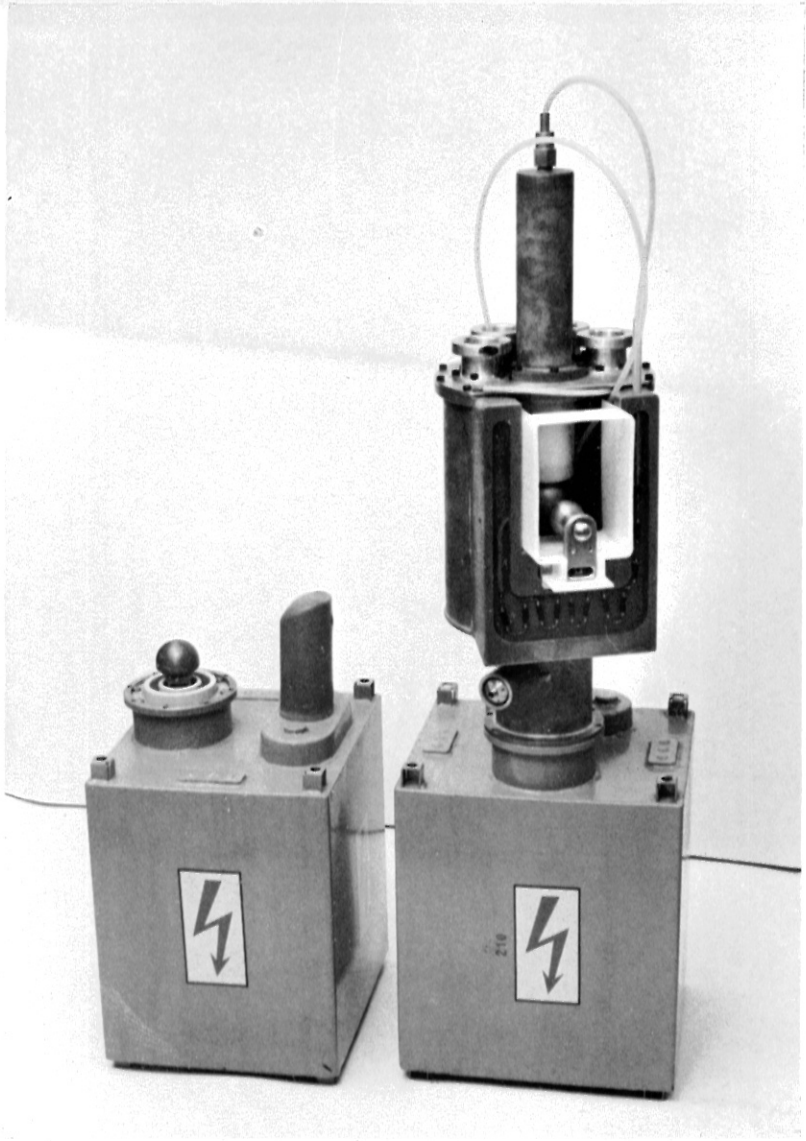

H 074 energy storage capacitor

2,6 µF 40 kV

coaxial termination with main electrode and charge termination

with combined start crowbar spark gap

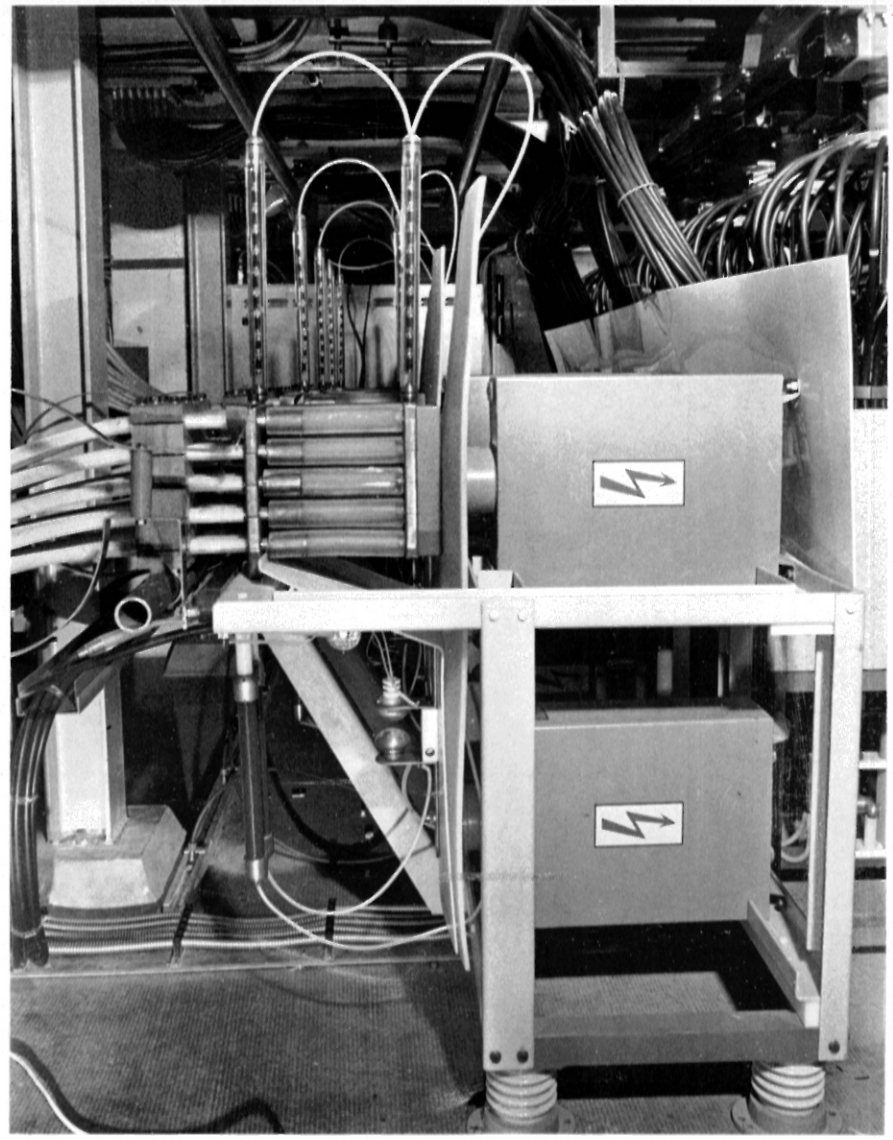

H 094

five installed marx generators to trigger one half of the bank

data of one circuit

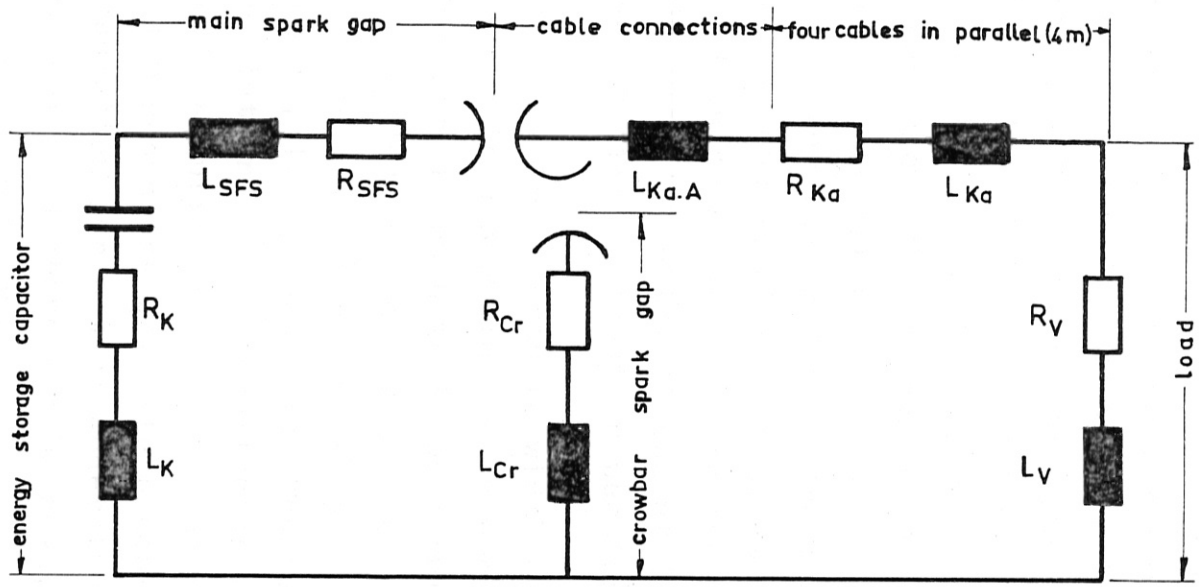

$L_K = 40 \cdot 10^{-9}$ H

$L_{SFS} = 40 \cdot 10^{-9}$ H

$L_{KaA} = 40 \cdot 10^{-9}$ H

$L_{Ka} = 125 \cdot 10^{-9}$ H

$L_V = 735 \cdot 10^{-9}$ H

$L_{Cr} = 180 \cdot 10^{-9}$ H

$R_K = 16 \cdot 10^{-3} \Omega$

$R_{SFS} = 8 \cdot 10^{-3} \Omega$

$R_{Ka} = 1.52 \cdot 10^{-3} \Omega$ (dc)

$R_{Ka+V} = 20 \cdot 10^{-3} \Omega$ (100 kc/s)

$R_{Cr} = 7 \cdot 10^{-3} \Omega$

H 096

5.4 The collector system

The collector had to be designed very flexible because of a possible change from a double fed linear to a single fed toroidal load. So it was composed of single precollectors each comprising two collector elements, according to fig. P 111. These two elements form a double T-profile which serves as a mechanical support. Figure P 135 is a cross-sectional view, which shows the current conducting copper sheets, the backing plates and the spanning wedges, as well as the sliding contacts for the cables. Correct mounting required a subdivision of the copper plate. Thus, at first, the mechanical adjustment is done, after which the contacts are fixed. Because of the very low pulse stress at the contact line, these contacts remain fixed without inspection.

The ratio of length to width of the precollector current sheets is chosen to give approximately minimum inductance. The form is such that local current density concentration is avoided, especially at the edge leading towards the overlap region, where the U-bend precollector insulation (mylar sheets, 1.2 mm total thickness) touch the main collector insulation. Each precollector includes connectors for two voltage suppresser units, one below, one above. Picture P 130 shows one complete precollector with partially cut insulation for better understanding. The precollector design as mentioned above can be seen, together with some cables in their position.

On each side of the double fed coil, 10 precollectors have been stacked, the whole package hanging in a support frame and being compressed in horizontal direction. After adjustment, the main collector plates were added.

As the bank energy can be varied in fifths, the main collector plates are fitted with appropriate curvature radii in order to allow the partial performance from the point of view of current density distribution.

The overlap, main collector and coil regions are held against electromechanical pulse force by an inclined spanning frame exerting about 5% of the peak pulse force: picture P 129. Thus the movement of the main collector plates is some tenths of a millimeter. All contact elements have been made from Cu/Cr.

The earth connection for the double fed coil was made by a short circuit winding at both coil ends which because of flux return is linked with nearly zero flux and thus fulfil the condition that both bank halves should be earth connected to the same point.

One precollector half has been life-tested in a voltage test as well as with original discharge conditions produced by six capacitor bank units. The voltage test ran over 20.000 shots at 98 kV peak-to-peak; furthermore, 2.500 crowbarred 40 kV shots were executed.

The mechanical adjustment of the precollectors has to be carried out very carefully, especially where high local field pressure occures at separate current conducting sheets, unless the hammering effect reported after about will begin.

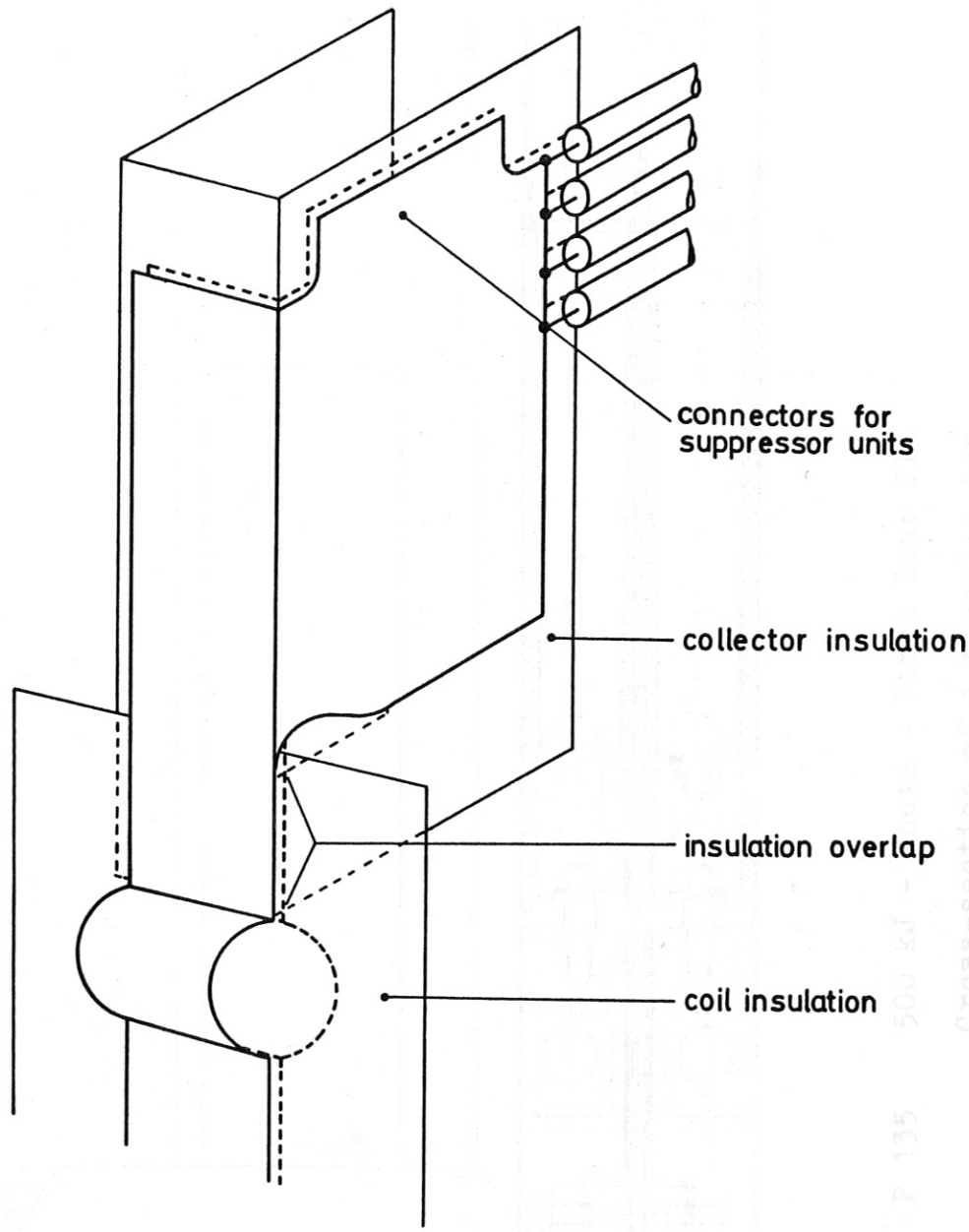

P 111 Collector section

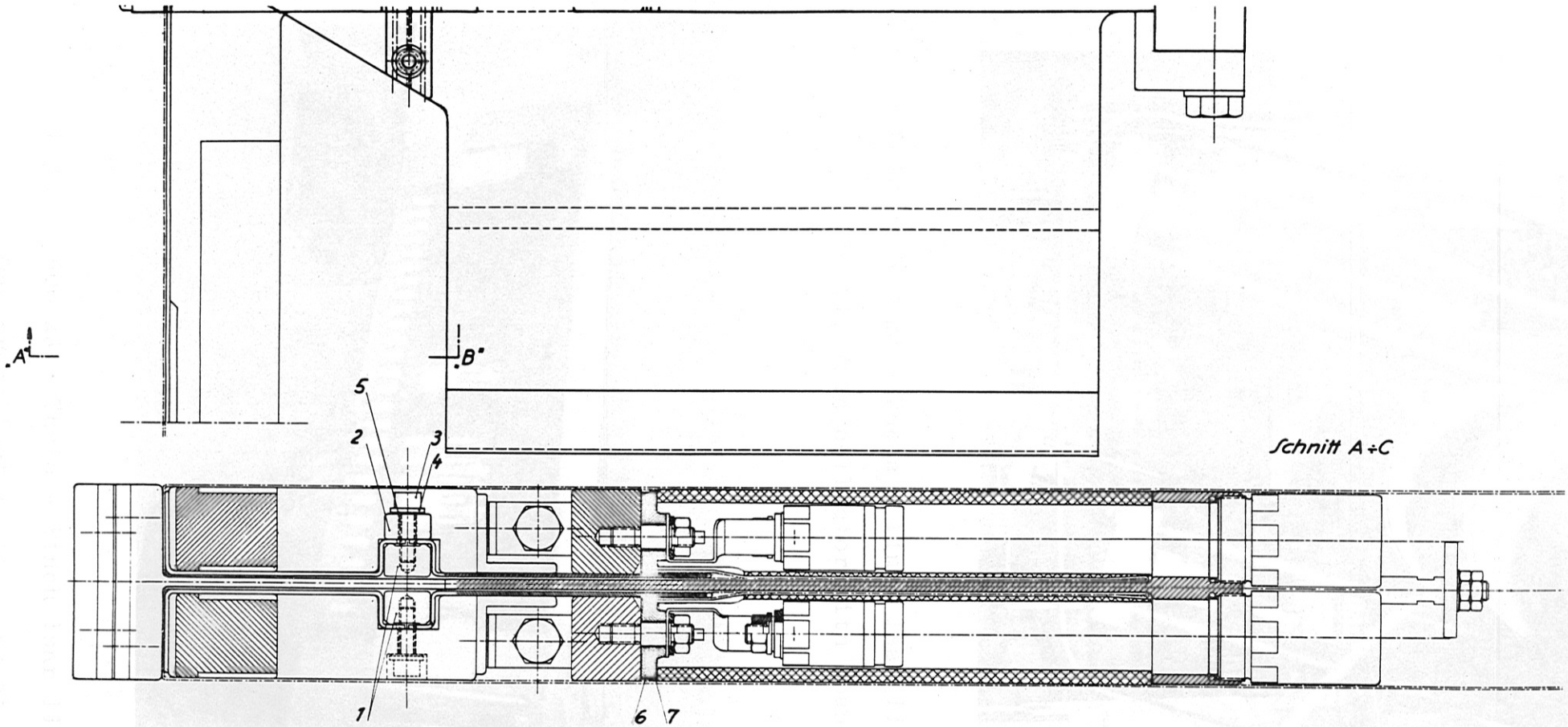

P 135 500 kJ - Theta - Pinch Isar II

Cross-section of a precollector

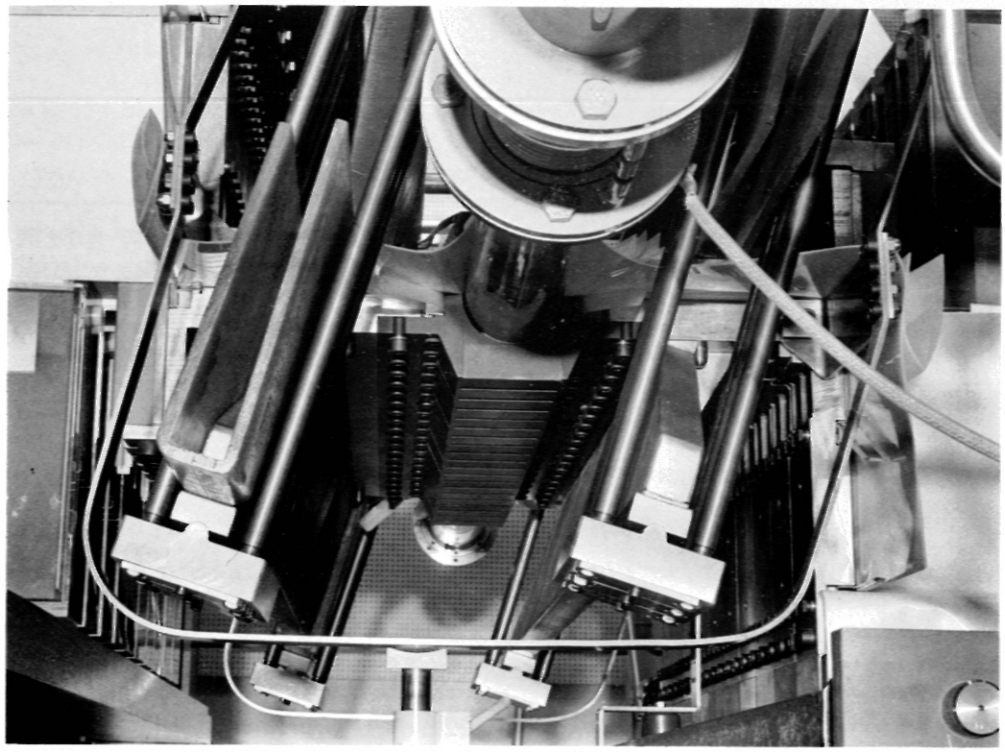

P 129 500 kJ - Theta - Pinch Isar II

Coil, main collector with spanning

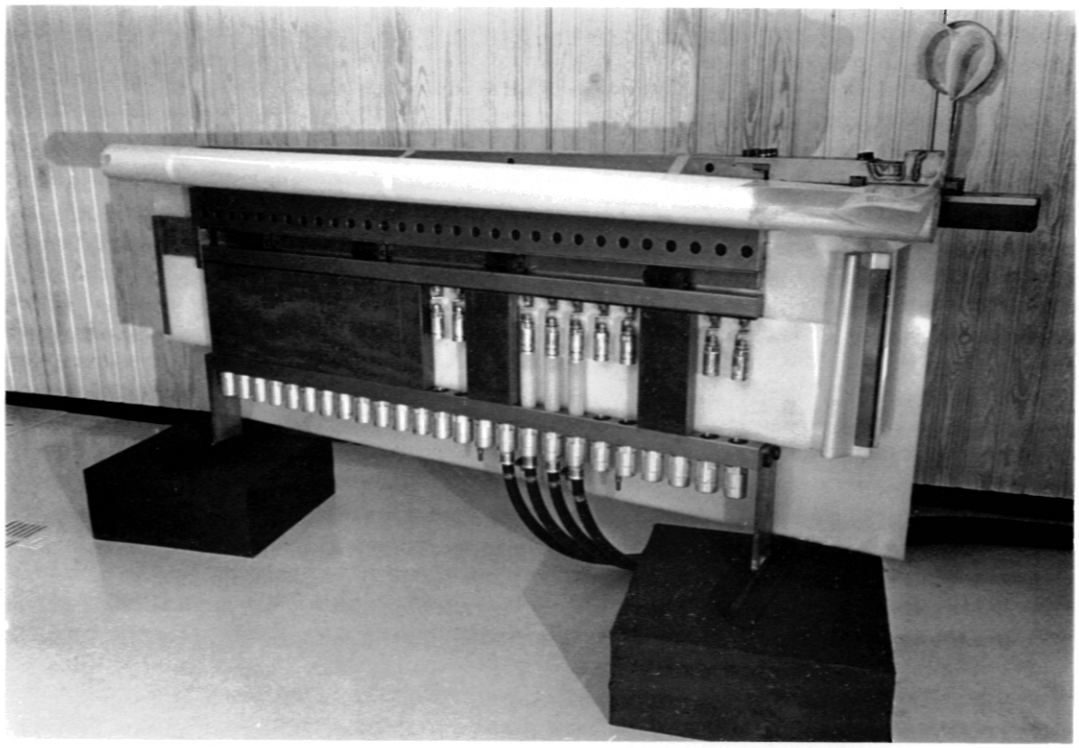

P 130 500 kJ - Theta - Pinch Isar II

One precollector with insulation
partially cut off

5.5 The R.-C. Transient suppression unit (Figure H 073)

To prevent overvoltages by reflections on the unterminated coaxial load-cables suppression units are mounted to the precollectors, containing a concentrated capacitance with a resistor in series. For optimum effect, the capacitance must be independent of voltage and frequency as far as possible. Therefore, a dielectric of paper was not applicable, because the dielectric constant of impregnated paper decreases above 1.5 to 2 MHz, according to the impregnation fluid used. Ceramic as a dielectric has two important disadvantages. Firstly, the dielectric constant depents on the electrical stress and secondly manufacture is difficult, especially at high voltages, when series circuits are necessary. Hence foils of plastic were taken, with a dielectric constant practically independent of the stress and nearly independent of the frequency, at least in the demanded range.

Due to the dimensions of the units, they must be connected close to the precollector where the space is very restricted, they would not be built in a conventional winding construction. So the plastic foils were piled up, being held together externaly by two copper plates, which also served as the contacts. There were five groups in series, each with 41 branches in parallel.

The resistor connected in series with the capacitor is made of megapyr (ϱ = 1.4 $\Omega mm^2/m$) as a compressed zig-zag with an insulation of mylar foils. Capacitor and resistor wer assembled in the same case, witch was constructed out of perpex (plexiglas). The cover of the case was made of epoxy resin into which a wide parallel plate termination was moulded.

The whole unit is carefully impregnated with a special mineral oil of low viscosity, so that the starting ionisation voltage is higher than the working voltage.

The electrical data of the suppression unit are:

capacitance	$C = 96\ nF \pm 1\%$
inductance	$L \leq 3\ nH$
maximum voltage	$U_m = 55\ kV_p$
resistance	$R = 888\ m\Omega$
life expectance at U_m	$\geq 5 \times 10^5$ pulses

Capacitance and resistance are nearly independent of voltage and frequency in the range of 1 kV to 55 kV and 100 kHz to 5 MHz.

R. C. Kunze

5.6 The voltage sensing system

With the aid of a voltage sensing system, defective capacitors (for instance short circuited) and units disconnected from the charging line can be found and registered. The capacitors have been combined into groups of six with a common load resistor, (c.f. figure P 128); the bank consists of 2 x 20 such groups. The voltage at each of these groups of six is measured and compared with the voltage of one leading group. If one capacitor is shorted or if it is disconnected at the charching terminal, a potential difference occurs during charging between this defective group and the leading group. When the potential difference rises above a certain threshold, which is fixed with respect to the minimum fault possible, charging is stoped and the defective group will be indicated at the control panel. The bank then must be earth connected by a safety discharge. Two racks belonging together are fitted with one leading group. The entire installation has 2 x 5 leading groups which can be selected from the control panel. A fault occuring at the same time in all operating groups and the corresponding leading group is not indicated because no potential difference occurs.

The probability of such a fault without indication is calculated as follows.
Within a guaranteed life of 25.000 discharges 10% defective capacitors are tolerable. As the wiring of the units after the end of the assembly has been checked in detail, disconnections of charging lines would scarcely occur.

The fault probability of one capacitor is given by p_c=10%, the fault probability for a group of six capacitors is

$$p_g = 1 - (1-p_c)^6 = 46.85\%$$

The fault probability for N capacitors operating, that is N/ 6 groups, is

$$p_N = p_g^{N/6}$$

1) 2/5 - performance

per bank half N = 48

$p_{2/5} = p_g^{8} = 23 \times 10^{-4}$

2) 1/1 - performance

per bank half N = 120

$p_{1/1} = p_g^{20} = 2.56 \times 10^{-7}$

Within the rated life of 25.000 discharges, there are 58 cases which will not be indicated in 2/5 - performance, and a negligible number (6.4×10^{-3}) of unindicated faults in the 1/1 - performance, since the fault probability of each capacitor is 10%.

The sensor used for the system is an ohmic voltage divider with an upper resistance of 80 MΩ . Thus we have the following circuit diagram for a single rack, see figure P 131.

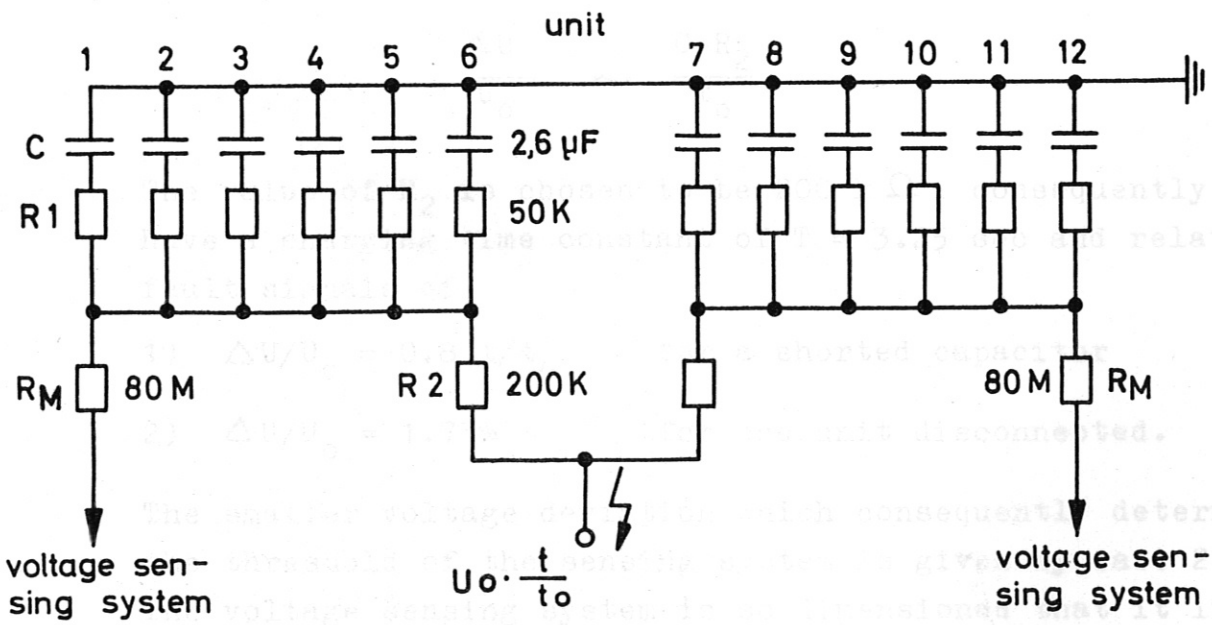

P 131

The discharge decay constant, T, is given by

$$T = (R_2 + R_1/6) \cdot 6C$$

The decoupling resistor, R_1, is fixed at $R_1 = 50\ k\Omega$ and R_2 is chosen with respect to the charging constant and the fault indication.

For a charging time of $t_o = 30$ sec, a charging time constant for constant current charging of about 3 sec is chosen.

$$(R_2 + R_1/6)\ 6C = 3 \text{ sec}$$

$$R_2 + R_1/6 = 192\ k\Omega \quad ; \quad R_2 = 184\ k\Omega \ .$$

For $T \ll t_o$ the relative fault signal of one defective group compared to the corresponding leading group is given by

1) for a shorted capacitor,

$$\frac{\Delta U}{U_o} \sim \frac{R_2}{R_1 + R_2} \cdot \frac{t}{t_o}$$

2) for one unit disconnected,

$$\frac{\Delta U}{U_o} \sim \frac{C \cdot R_2}{t_o}$$

The value of R_2 is chosen to be $200\ k\Omega$, consequently we have a charging time constant of $T = 3.25$ sec and relative fault signals of,

1) $\Delta U/U_o = 0.8\ t/t_o$ for a shorted capacitor

2) $\Delta U/U_o = 1.73\%$ for one unit disconnected.

The smaller voltage deviation which consequently determines the threshold of the sensing system is given by case 2) . The voltage sensing system is so dimensioned that it indicates a potential difference of 1% between the leading group and the other group.

Corresponding to the tolerances of the elements used, a possible potential difference between two groups with one disconnected unit each turnsout to be

$$\frac{\Delta C \cdot R_2 + \Delta R_2 \cdot C}{t_o}$$

In the present installation the maximum fault of this kind which can occur is 0.0675 %. The choice of 1 % for the threshold allows sufficient safety.

The upper resistor of the voltage divider is arranged in one of the six corresponding tiers of the bank. On the other hand the lower resistor, amplifiers, rectifiers, discrimination sets, relais and other apparatus of the measurement electronics and the fault indicators are mounted in the control desk.

5.7 The bias field bank

The bias field bank was composed of the same units as were used for the project " Turbulence Heating Experiment", see report 4/50 (Institut für Plasmaphysik).
Two halves of the bias field bank consists of 5 units each and can be operated at partial energy in the same way as the main bank. The bias field bank operates at 12 kV charging voltage. Therefore, disconnecting switches for the single units were necessary in order to disconnect the bias field bank in cases where it is not used. In order to avoid overvoltages due to cable reflections at the bias field bank cable ends with open disconnecting switches, electrolytic resistors, of the approximate resulting characteristic impedance of the cables, are connected across the cable terminals.

The bias field bank has the following data:
(Data for one half bank)

Capacitance	145 /uF
Inductance	0.86/uF
Resistance	6.1 m Ω
Charging voltage	12 kV
Peak current	148 kA
Frequency	14 kHz
Crowbar time constant	225 /u sec

P 133 500 kJ - Theta - Pinch

Submaster sparkgap

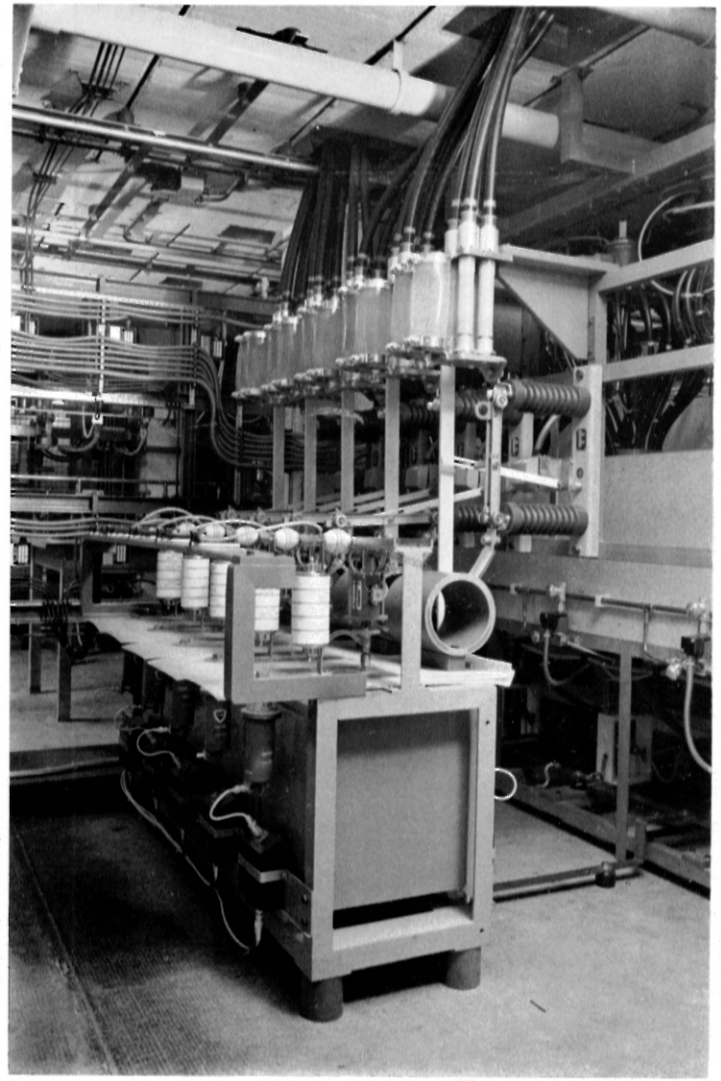

P 134 500 kJ - Theta - Pinch

One half of the
bias field bank

5.8 Control and electronics desk

The control of the whole installation is operated from the control panel, which together with the Faraday cage, has been arranged in a separate room beside the experimental hall, c.f. figure P 132.

The main section of the control panel is occupied by the operating elements for the slow control functions: put in control supply switch, preselection of desired performance (with or without crowbar, bias field, preionisation), control of shorting breakers and corresponding charging power supplies and in case of emergency discharge of the bank via the charging resistors.
In the right hand section of the control panel the electronic trigger sets have been mounted together with the corresponding power supplies and time delay units. The upper part of the control desk contains the voltage sensing system, the indicateing lamps and push buttons for reference voltage selection.

Several interlocking circuits have been provided in order to give safety protection for the operating personnel and the installation itself.
Switching on the control voltage supply all doors leading to the experiment - if closed - will be electrically interlocked. The shorting breakers can only be opened if the following conditions are accomplished; all doors must be closed and interlocked, the electric crane and the mounting carriage must be out of the bank region and the air pressure must be high enough. The position of the shorting breakers is monitored by micro switches. The charging power supplies can only be switched on if the corresponding shorting breakers are opened.

Pushing one of the emergency buttons, which are mounted on the control panel and at several points of the installation, causes an immediate shutting of all shorting breakers.

Pushing the emergency buttons is equivalent in violence to one of the conditions for the shorting breakers to be opened. Further interlocking circuits in the control system check that, for both bank halves in a correct position of the disconnecting switches, the same kind of performance has been chosen. For instance, for partial performance at both sides of the bank, the corresponding disconnecting switches must be put in; in crowbar operation, the corresponding crowbar disconnecting switches are put in in the same way.

The bias field bank is switched with ignitrons in the same sense as the main bank. The position of the disconnecting switches belonging to the halves of the bias field bank is checked by means of an interlocking circuit.

Should any disturbance of symmetry of both halves of the installation occur, then the charging will be disconnected. A monitoring table over the control desk will indicate the fault. The symmetry conditions mentioned above also hold for a single fed toroidal coil if, the minimum partial energy stage in this arrangement is one fifth.

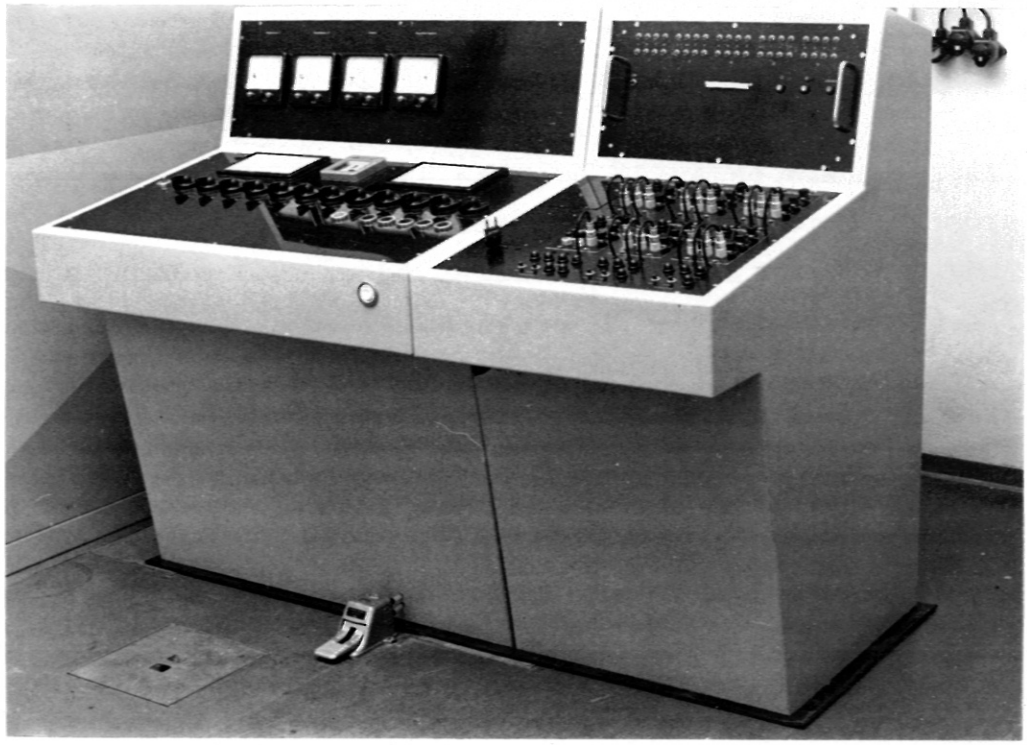

P 132 500 kJ - Theta - Pinch Isar II

Control desk

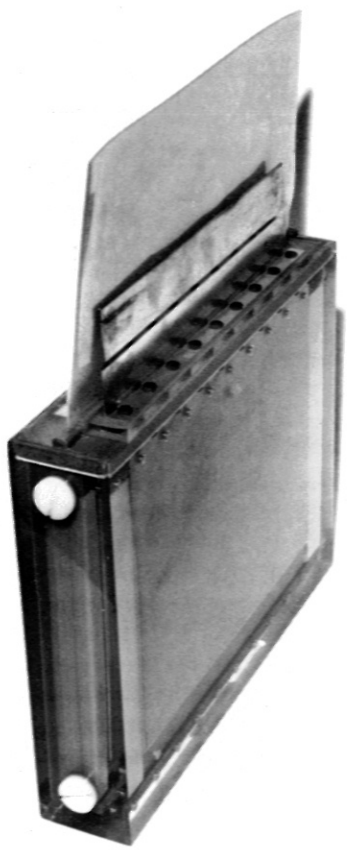

H 073

500 kJ - Theta - Pinch

R-C transient suppression-unit 96 nF, 0,888 Ohm

6. Assembling the system with the aid of general job planning

In 1965 the 500 kV-installation Isar II was planned. In the first two years all activities were prepared with the aid of dash diagrams. In the course of the work, an increasing overlap of development and manufacture occured. From the beginning of 1967 network analysis of the general job planning was applied to this project.

Report IPP 4/45 describes the different job planning methods for instance PERT, CPM, MPM and compares than.
It appeared to us that the metra potential method (MPM) would be the best suited for projects like this. The MPM method, which has the following properties, was used.

In the so called network the activities are represented by nodes and the logical connections between these nodes are called paths, which are represented by arrows. The nodes indicate the beginning of an activity and the time difference between the beginning of two activities is called length of the path. It is possible to represent this length by the length of the arrow or of its projection on the time axis. Usually the value of path length is written on the arrow and its geometrical length has no connexion to time. The maximum time difference tolerable between the beginning of two activities is indicated by a negative sign. If two activities are to begin at the same time, they must be connected with an arrow of zero length.

The total path with the maximum length is the critical path, which determins the end of the project.
In figure P 136 are:

A, B, C, D = activities
a+d, b+c+d = total pathes
a = difference of beginnings of A and B
α = duration of the activity A

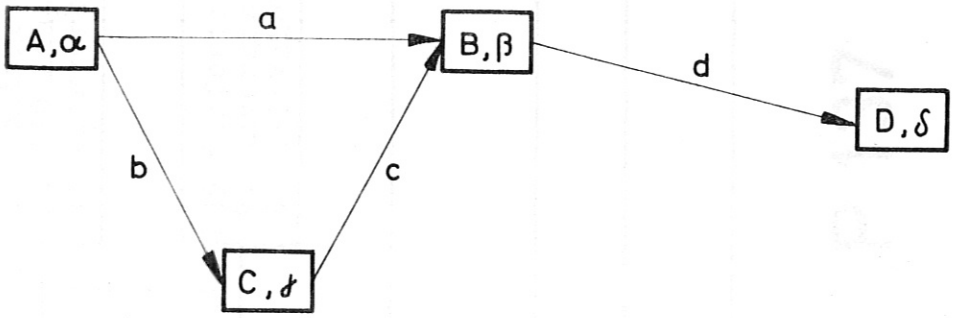

P 136

From figure P 136, the following calculation method results:
The beginning time t_A of A is the beginning.

The beginning time t_B of B is calculated from,

$$t_B = \max (t_A+a, t_A+b+c) ,$$

likewise $t_D = t_B+d$

The project end t_E is determined by

$$t_E = t_D+ \delta$$

Normaly the following conditions hold:

$a \geq \alpha$ $\qquad$ $c \geq \gamma$
$b \geq \alpha$ $\qquad$ $d \geq \beta$

Two activities can also overlap in their durations, that is a second activity (for instance D) can begin before the first one (B) has ended. In this case, d becomes less than β .

The network for the 500 kJ bank consists of about 100 activities. A small section including 13 activities is shown in figure P 137.
The following figure, P 138, shows the graphical representation of one activity with the following informations:
name of the activity (Text); number in the network; expert; duration of the activity; buffering time (time difference between the latest and the earliest beginning).

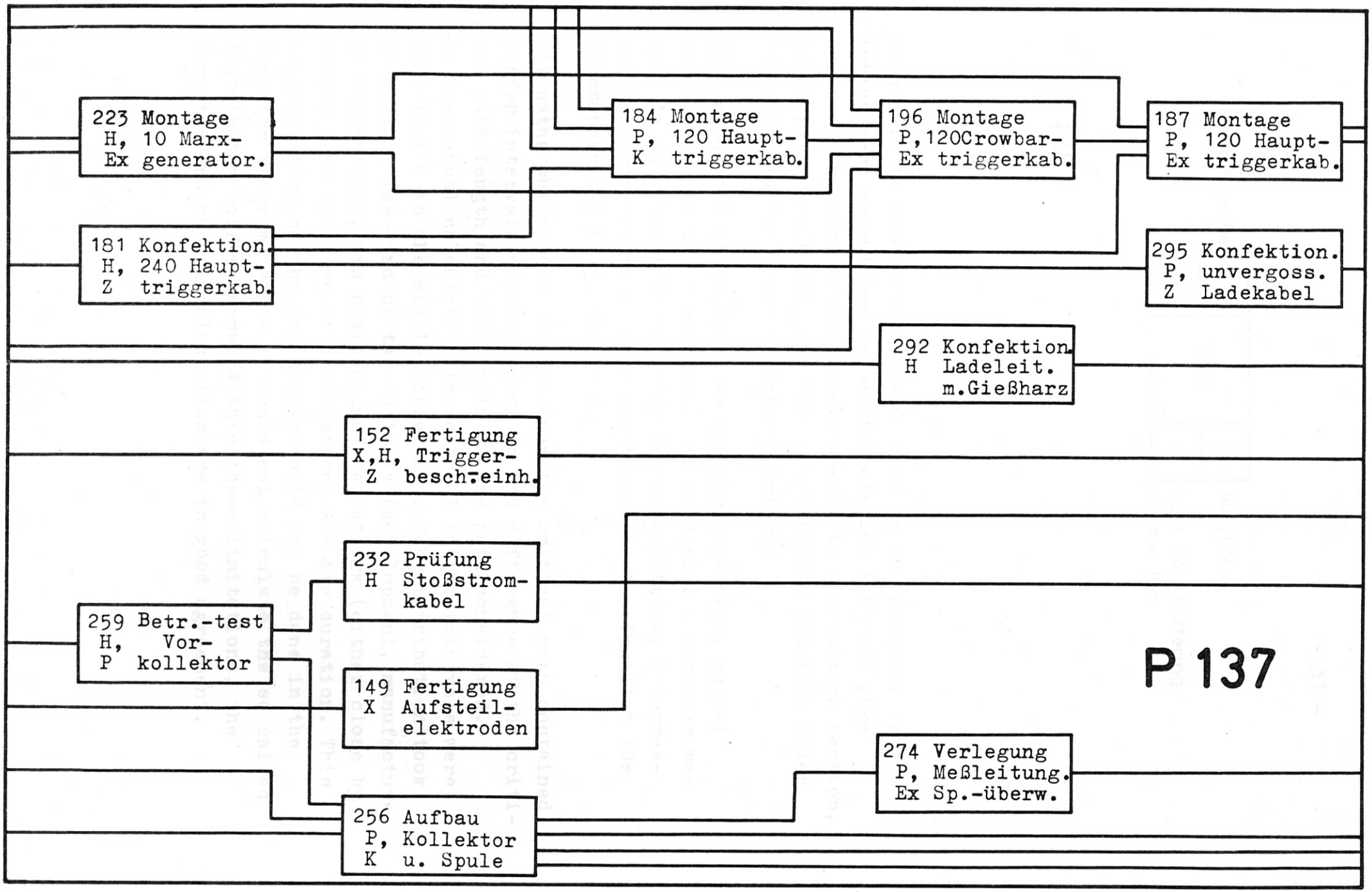
223 Montage H, 10 Marx- Ex generator.
184 Montage P, 120 Haupt- K triggerkab.
196 Montage P,120Crowbar- Ex triggerkab.
187 Montage P, 120 Haupt- Ex triggerkab.
181 Konfektion. H, 240 Haupt- Z triggerkab.
295 Konfektion. P, unvergoss. Z Ladekabel
292 Konfektion. H Ladeleit. m.Gießharz
152 Fertigung X,H, Trigger- Z beschr.einh.
232 Prüfung H Stoßstrom- kabel
259 Betr.-test H, Vor- P kollektor
149 Fertigung X Aufsteil- elektroden
274 Verlegung P, Meßleitung. Ex Sp.-überw.
256 Aufbau P, Kollektor K u. Spule
P 137

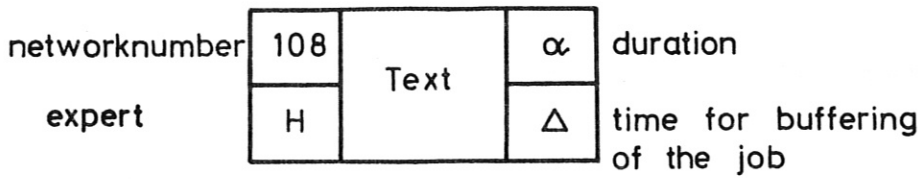

P 138

As an aid to the experts taking part in the project, term tables were calculated and distributed.On the next page parts of the term tables corresponding to the network section, shown in figure P 137, had been selected and put into order according to the three experts concerned.

With about 100 activities, as was the case here, manual calculation of the terms was still possible. A computer was used in an attempt to simplify the calculations. A corresponding program was written and tested in the Institut für Plasmaphysik (by H. Becker).

All paths which were shorter than the critical path contained buffer intervals corresponding to the difference of the critical path length and the length of the path considered.
In the manual calculation these total buffer intervals were distributed to the single activities. The distribution took account of the kind of the activity (development, manufacture or assembling), its position in the network (either close by or far from the time of calculation) and its duration. This qualification of the activities could not be done in the computer program, since it could not calculate the so called distributed buffer terms. Within these limitations, the computer and manual calculation are in good agreement.

Tätigkeitsliste

Auftrag Nr. 1B - P 0701

Aktenz. Nr. 201.5/ 15

Bearbeiter	Netzplan Nr.	Tätigkeit	Dauer Woch.	frühester Beginn	spätester Beginn	spätes Ende	Pufferzeit Woch.	Bemerkungen
Bearbeiter: Projektierung (P)								
P, K	184	Montage 120 Haupttrigg.kabel	2,4	22.6.	22.6.	7.7.	0	
P, Ex	196	Montage 120 Crowbartrigg.kabel	2,6	17.7.	21.7.	8.8.	0,8	
P, Ex	187	Montage 120 Haupttrigg.kabel	2	9.8.	17.8.	30.8.	0,8	
P, K	256	Aufbau von Vorkollektoren und Hauptkollektor und Spule	4	2.8.	9.8.	7.9.	1	
P, Z	295	Konfektionierung der unvergoss. Ladekabel (25 Stück)	1,4	14.6.	24.8.	1.9.	9,8	
P, Ex	274	Verlegung der Meßleitungen zur Spannungsüberwachung	2	8.9.	6.11.	17.11.	8	
Bearbeiter: Hochspannunstechnik (H)								
H, Z	181	Konfektionierung von 240 Haupttriggerkabeln	4,8	22.5.	22.5.	23.6.	0	
H, Ex	223	Montage von 10 Marxgeneratoren mit Gestellen	3,2	19.6.	19.6.	11.7.	0	
H, P	259	Betriebsm. Test eines Vorkoll. im 6 Kreis - Versuch	3,2	26.6.	18.7.	1.8.	3,2	
H	292	Konfektionierung von 34 Ladel. mit Gießharzendenabschluß	9	21.6.	29.6.	1.9.	1,2	
H	232	Prüfung von 16 Stoßstromkabeln im 6 Kreis - Versuch bei 10.000 Entladungen	3,4	16.8.	16.8.	7.9.	0	
Bearbeiter: mechanische Zentralwerkstatt (X)								
X	149	Fertigung 240 Aufsteilelektr.	2,6	2.8.	31.10.	17.11.	12,4	
X,H,Z	152	Fertigung Triggerbeschaltungseinheit (240 Stück)	6	27.7.	25.8.	5.10.	3,8	

After the end of the assembly, the results of the planning methods were compared with and without the job planning technics. The essential advantages seem to be the following.

The influence of term shifts on the entire project can be checked at once. Free manpower, or manpower becoming available, was ascertained and was used in order to avoid delay.
We realised that the special symmetric arrangement of the system was often useful to subdivide the actual task into two independent activities.
Finally, we often took advantage of partial overlap of several consecutive activities.

In general one can say that we obtained an improved survey and a better coordination of the activities, better information of all people involved and therefore, a highter effectivity of the sources given with regard to manpower, machines and space.

This work was performed under the terms of the agreement on association between the Institut für Plasmsphysik and EURATOM.

Acknowledgments:

The work reported was performed mainly by members of the Engineering Division, headed by K. H. Schmitter, including the assistance of some industrial firms.

The authors wish to acknowledge the collaboration of the following colleagues whose names do not appear in the various reports presented in the conference:

J. Gruber, E. Hecht, G. Kaspar, M. Kottmair, J. Leinthaler, K. Maischberger, E. Ring, H. Stoll, A. Wasner, H. Weichselgartner, G. Wulff

References:

1) "Low - Inductance Switching Using Parallel Spark-Gaps
R.A. Fitch, N.R. McCormick
Convention on Thermonuclear Processes 1959

2) "Combined Start Crowbar Spark Gap with wide Operating Range"
H. Hägelsperger, G. Klement, R.C. Kunze, G. Müller
Report 4/28 1966 Insitut für Plasmaphysik, Garching

3) "Pressurised Switching Unit"
G. Müller
Report 4/52 1968 Institut für Plasmaphysik, Garching

4) "Über eine einfache Kurzschluß-Funkenstrecke für Stoßstromanordnungen"
R. Wilhelm, H. Zwicker
Zeitschrift für angewandte Physik 1965

5) "Ferrite decoupled Crowbar Spark Gap"
H. Wedler, E. v.Mark, R.C. Kunze, G. Klement
Report 4/32 1966 Institut für Plasmaphysik, Garching

6) "Crowbar System at Isar I "
E. v.Mark, H. Wedler
Report 4/59 1968 Institut für Plasmaphysik, Garching

7) "Power Crowbar of Low Inductance Capacitor Banks using Atmospheric Spark Gaps"
N.R. McCormick, D. Markuss, L. Firth
Report CLM - P127 1966 Culham Laboratory

8) "Tests on a Master Gap working at Atmospheric Pressure"
D.V. Bayes
Report 4/40 1967 Institut für Plasmaphysik, Garching

9) " 15 kV Triggergerät mit Funkenstrecke "
E. v.Mark, R.C. Kunze
Report 4/43 1967 Institut für Plasmaphysik, Garching

10) "Impulskondensatoren"
R.C. Kunze
Report 4/35 1967 Institut für Plasmaphysik, Garching

11) "New Fast Capacitor Banks for Theta-Pinch-Experiments at the Institut für Plasmaphysik in Garching"
K.H. Fertl, G. Herppich, A. Knobloch, H. Schlageter
Report 4/26 1966 Institut für Plasmaphysik, Garching

12) "Capacitor Banks for a Turbulence Heating Experiment"
G. Herppich, A. Knobloch, G. Müller
Report 4/50 1968 Institut für Plasmaphysik, Garching

13) "Technical Experience with the Isar I Collector"
E. Breit, A. Knobloch
Report 4/56 1968 Institut für Plasmaphysik, Garching

14) " RC Transient Suppressor Units"
R.C. Kunze
Report 4/53 1968 Institut für Plasmaphysik, Garching

15) "An analog system for the design of switched discharge circuits in plasma physics"
G. Herppich, A. Knobloch
Report 4/29 1966 Institut für Plasmaphysik, Garching

16) "A Summary and Explanation of the Most Important Methods of the Network Analysis"
G. Nützel, R. Weiß
Report 4/45 1967 Institut für Plasmaphysik